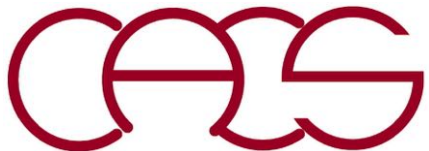


Quantum Molecular Dynamics Simulations

Aiichiro Nakano

*Collaboratory for Advanced Computing & Simulations
Depts. of Computer Science, Physics & Astronomy, Chemical
Engineering & Materials Science, and Biological Sciences
University of Southern California*

Email: anakano@usc.edu

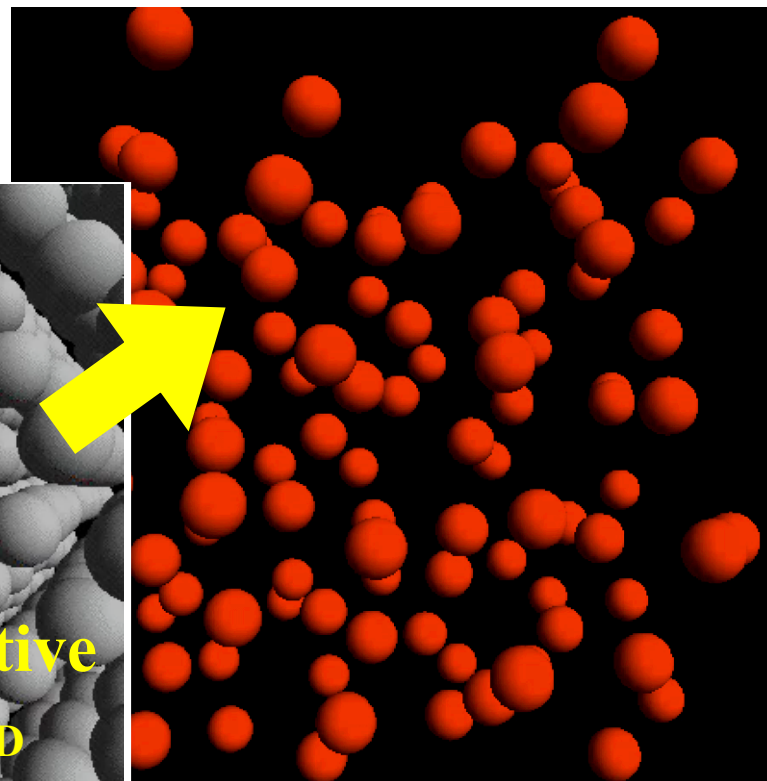
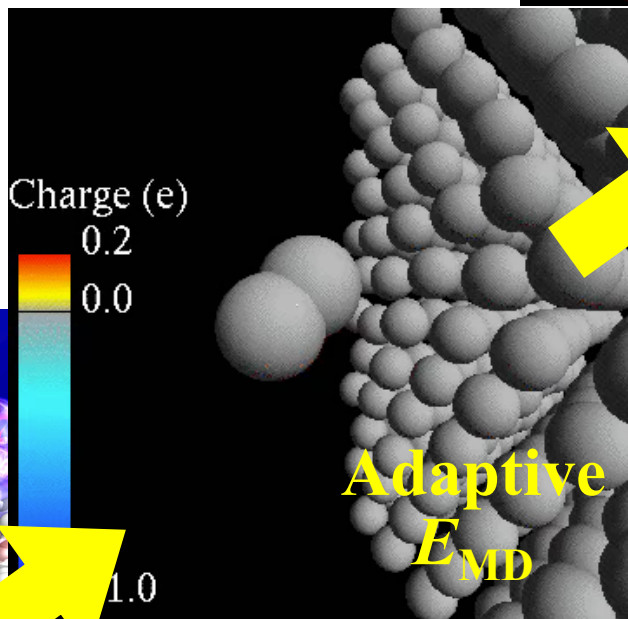
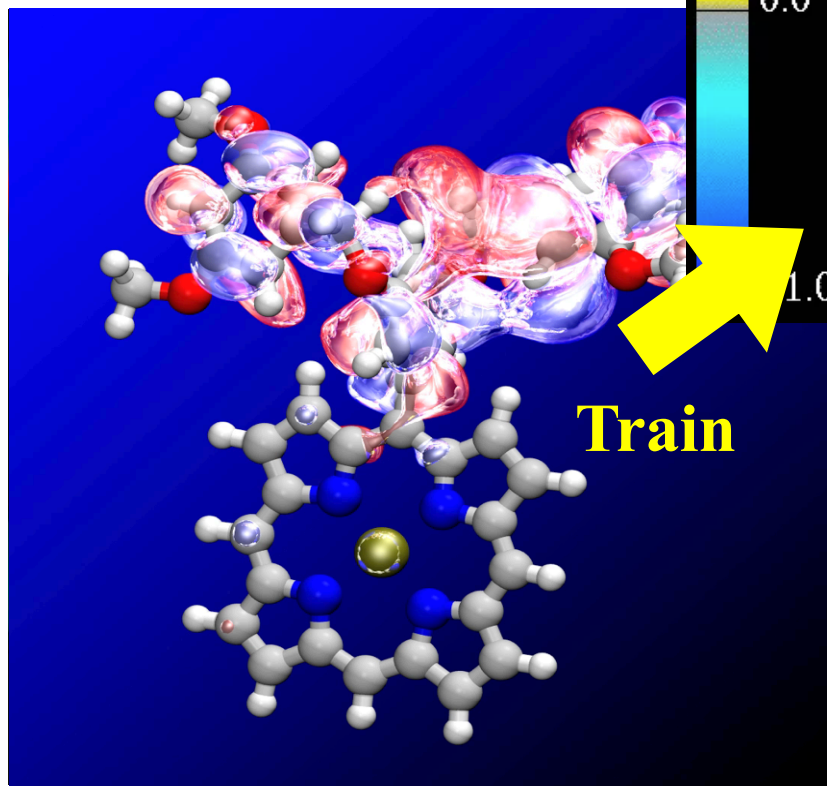


Molecular Dynamics Hierarchy

Molecular Dynamics (MD)

Reactive MD (RMD)

Nonadiabatic quantum MD (NAQMD)



First principles-based reactive force-fields

- Reactive bond order $\{BO_{ij}\}$
→ Bond breakage & formation
- Charge equilibration (QEq) $\{q_i\}$
→ Charge transfer

Quantum Molecular Dynamics (QMD)

$$M_I \frac{d^2}{dt^2} \mathbf{R}_I = - \frac{\partial}{\partial \mathbf{R}_I} E[\{\mathbf{R}_I\}, \psi(\mathbf{r}_1 \dots, \mathbf{r}_N)] \quad (I = 1, \dots, N_{\text{atom}})$$

First molecular dynamics using an empirical interatomic interaction

A. Rahman, *Phys. Rev.* **136**, A405 ('64)

$$\psi(\mathbf{r}_1 \dots, \mathbf{r}_N) \leftarrow \operatorname{argmin} E[\{\mathbf{R}_I\}, \psi(\mathbf{r}_1 \dots, \mathbf{r}_N)]$$

Density functional theory (DFT)

Hohenberg & Kohn, *Phys. Rev.* **136**, B864 ('64)

W. Kohn, *Nobel chemistry prize*, '98

$O(C^N)$ \rightarrow $O(N^3)$
1 N -electron problem \rightarrow N 1-electron problems
intractable \rightarrow **tractable**

$$\psi(\mathbf{r}_1 \dots, \mathbf{r}_N) \quad \{\psi_i(\mathbf{r}) | i = 1, \dots, N\}$$

$O(N)$ DFT algorithms

- **Divide-&-conquer DFT** [W. Yang, *Phys. Rev. Lett.* **66**, 1438 ('91); F. Shimojo *et al.*, *Comput. Phys. Commun.* **167**, 151 ('05); *Phys Rev. B* **77**, 085103 ('08); *Appl. Phys. Lett.* **95**, 043114 ('09); *J. Chem. Phys.* **140**, 18A529 ('14)]
- **Quantum nearsightedness principle** [W. Kohn, *Phys. Rev. Lett.* **76**, 3168 ('96)]
- **A recent review** [Bowler & Miyazaki, *Rep. Prog. Phys.* **75**, 036503 ('12)]

Born-Oppenheimer Approximation

- Consider a system of N electrons & N_{atom} nuclei, with the Hamiltonian

$$\begin{aligned}
 \tilde{H} &= \sum_{I=1}^{N_{\text{atom}}} \frac{\mathbf{P}_I^2}{2M_I} + H(\{\mathbf{r}_i\}, \{\mathbf{R}_I\}) \\
 &= \sum_{I=1}^{N_{\text{atom}}} \left[\frac{\mathbf{P}_I^2}{2M_I} + V_{\text{ext}}(\mathbf{R}_I) \right] + \sum_{i=1}^N \left[-\frac{\hbar^2}{2m} \frac{\partial^2}{\partial \mathbf{r}_i^2} + v_{\text{ext}}(\mathbf{r}_i) \right] \\
 &\quad + \frac{1}{2} \sum_{i \neq j} \frac{e^2}{|\mathbf{r}_i - \mathbf{r}_j|} - \sum_{i,J} \frac{Z_J e^2}{|\mathbf{r}_i - \mathbf{R}_J|} + \frac{1}{2} \sum_{I \neq J} \frac{Z_I Z_J e^2}{|\mathbf{R}_I - \mathbf{R}_J|}
 \end{aligned}$$

nucleus momentum
electron position
nucleus position
nucleus charge

- Due to the much larger nuclei masses (M_I) compared to the electron mass (m), the quantum-mechanical wave function of the system is separable to those of the electrons & nuclei
- At ambient conditions, the electronic wave function remains in its ground state ($|\Psi_0\rangle$) corresponding to the instantaneous nuclei positions ($\{\mathbf{R}_I\}$), with the latter following classical mechanics

$$M_I \frac{d^2}{dt^2} \mathbf{R}_I = -\frac{\partial}{\partial \mathbf{R}_I} \langle \Psi_0 | H(\{\mathbf{r}_i\}, \{\mathbf{R}_I\}) | \Psi_0 \rangle$$

Complexity Reduction: Density Functional Theory

- **P. Hohenberg & W. Kohn, “Inhomogeneous electron gas”**

Phys. Rev. **136**, B864 ('64)

The electronic ground state is a functional of the electron density $\rho(\mathbf{r})$

- **W. Kohn & L. Sham, “Self-consistent equations including exchange & correlation effects”** *Phys. Rev.* **140**, A1133 ('65)

Derived a formally exact self-consistent single-electron equations for a many-electron system



Kohn-Sham Energy Eigenstates

- Time-independent Schrödinger equation

$$\begin{array}{ccc} \text{Hamiltonian} & \longrightarrow & H\psi_n(\mathbf{r}) = \epsilon_n \psi_n(\mathbf{r}) \longleftarrow \text{Eigenstate} \\ \text{operator} & & \text{Eigenvalue} \end{array}$$

- Stationary state

$$i\hbar \frac{\partial}{\partial t} \psi(t) = H\psi(t)$$

$$\psi(t) = \exp(-i\epsilon_n t/\hbar) \psi_n$$

- Hamiltonian operator

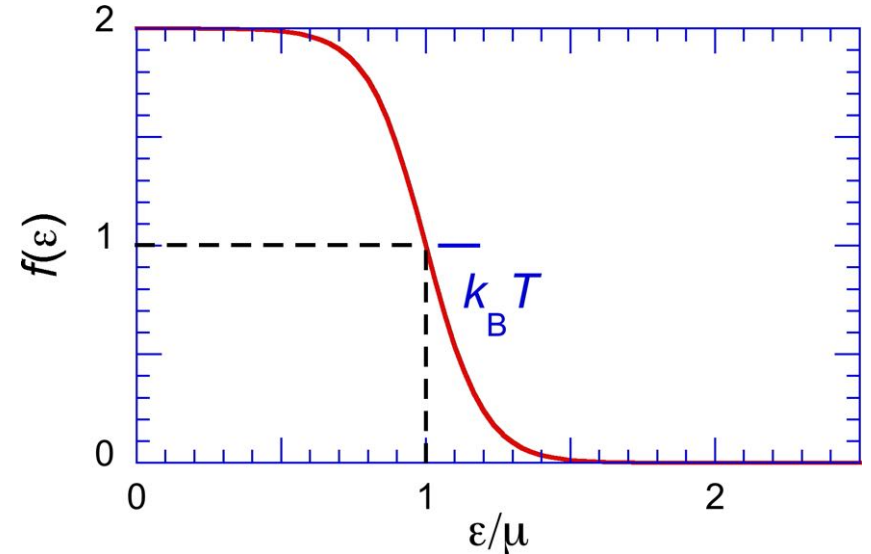
$$H = -\frac{\hbar^2}{2m} \frac{\partial^2}{\partial \mathbf{r}_i^2} + v(\mathbf{r})$$

- Density functional theory*

$$v(\mathbf{r}) = -\sum_I \frac{Z_I e^2}{|\mathbf{r} - \mathbf{R}_I|} + \int d\mathbf{r}' \frac{e^2 \rho(\mathbf{r}')}{|\mathbf{r} - \mathbf{r}'|} + v_{xc}(\mathbf{r})$$

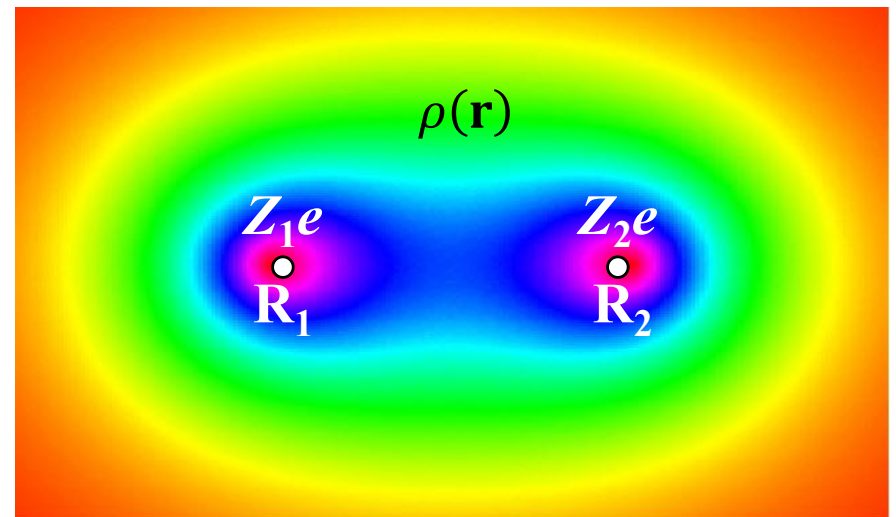
$$\rho(\mathbf{r}) = \sum_n \frac{2}{\exp\left(\frac{\epsilon_n - \mu}{k_B T}\right) + 1} |\psi_n(\mathbf{r})|^2$$

exchange-correlation potential



* $T = 0$ in Kohn-Sham'65; cf. Mermin

[Phy. Rev. **137**, A1441 ('65)]



Abstraction: Exchange-Correlation Functional

- **Universal functional (of density) that describes many-body effects beyond the mean-field approximation**

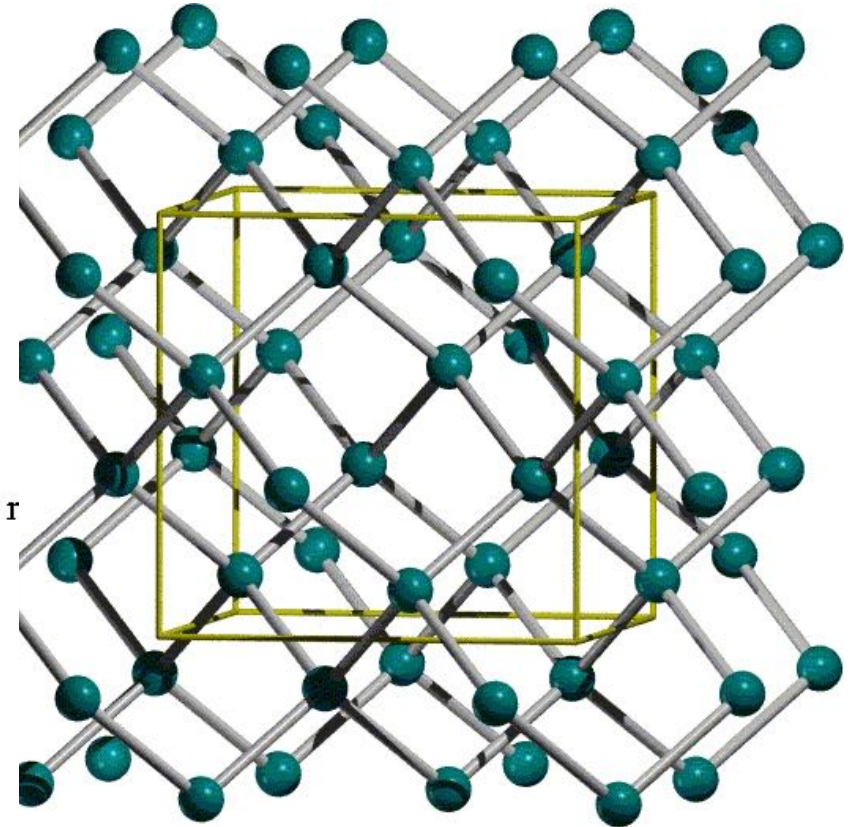
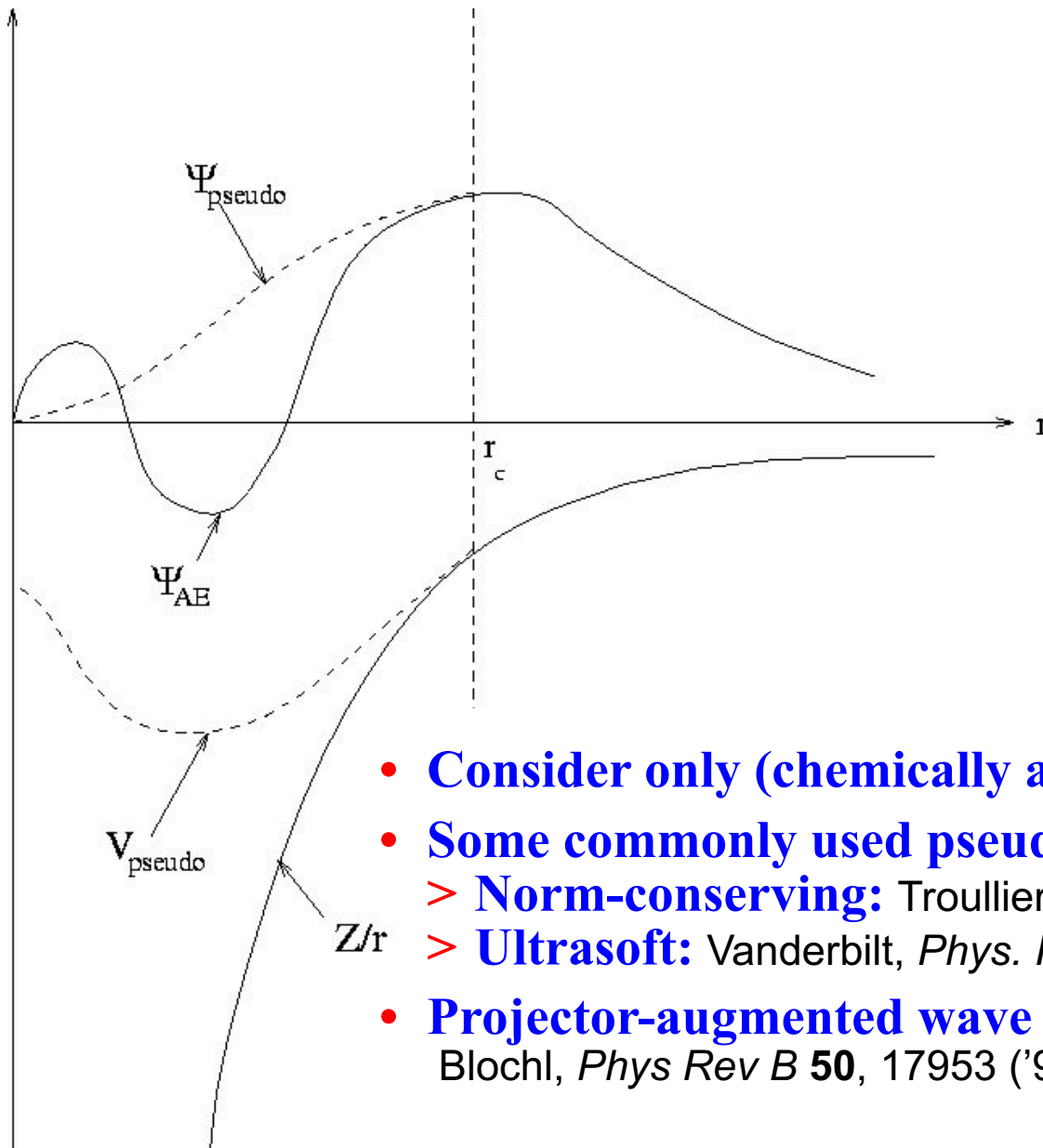
$$v_{\text{Hxc}}(\mathbf{r}) = \int d\mathbf{r}' \frac{e^2 \rho(\mathbf{r}')}{|\mathbf{r} - \mathbf{r}'|} + v_{\text{xc}}(\mathbf{r})$$

potential energy due to electron-electron interaction Hartree (mean-field) potential exchange-correlation potential

- **Some commonly used exchange-correlation functionals**
 - > **GGA (generalized gradient approximation)**
 - PBE:** Perdew, Burke & Ernzerhof, *Phys. Rev. Lett.* **77**, 3865 ('96)
 - > **MetaGGA**
 - SCAN:** Sun, Ruzsinszky & Perdew, *Phys. Rev. Lett.* **115**, 036402 ('15)
 - > **Hybrid exact-exchange (Hartree-Fock) functionals**
 - HSE:** Heyd, Scuseria & Ernzerhof, *J. Chem. Phys.* **118**, 8207 ('03)

Abstraction: Pseudopotential

- Silicon — $1s^2 2s^2 2p^6 3s^2 3p^2$



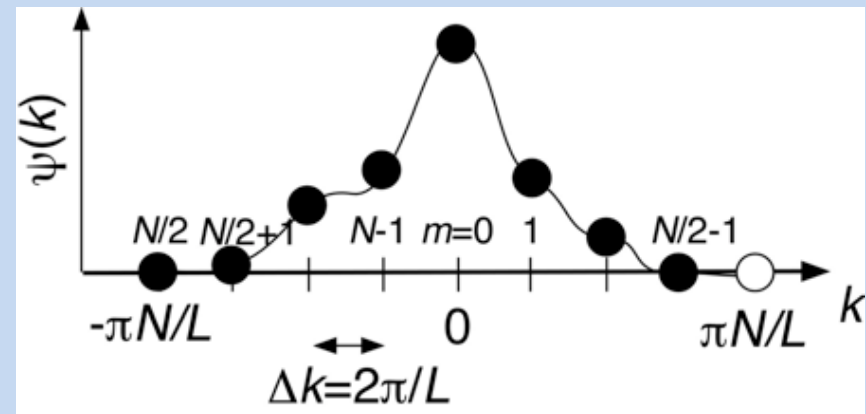
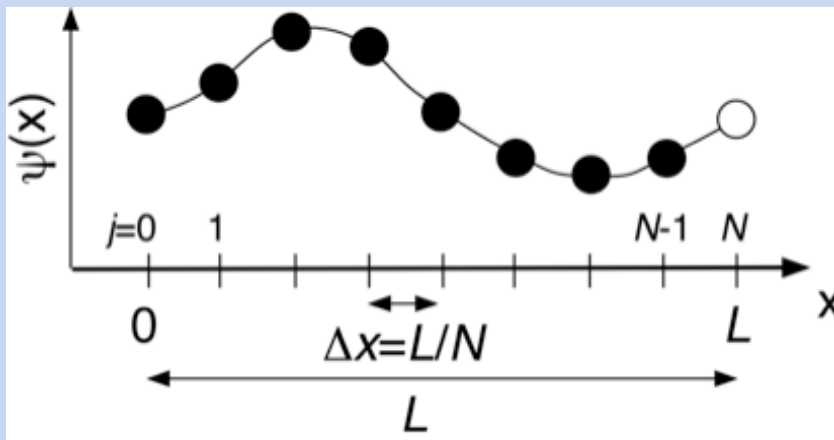
- Consider only (chemically active) valence electrons
- Some commonly used pseudopotentials
 - > Norm-conserving: Troullier & Martins, *Phys. Rev. B* **41**, 1993 ('91)
 - > Ultrasoft: Vanderbilt, *Phys. Rev. B* **41**, 7892 ('90)
- Projector-augmented wave (PAW) method
Blochl, *Phys Rev B* **50**, 17953 ('94)

Representation: Plane-Wave Basis

- Pseudopotentials result in slowly varying wave functions that can be represented on a regular grid, which in turn can be represented as a linear combination of plane waves, *i.e.*, Fourier transform

$$\psi(\mathbf{r}_j) = \sum_{\mathbf{k}_n} \psi_{\mathbf{k}_n} \exp(i\mathbf{k}_n \cdot \mathbf{r}_j)$$

1D example

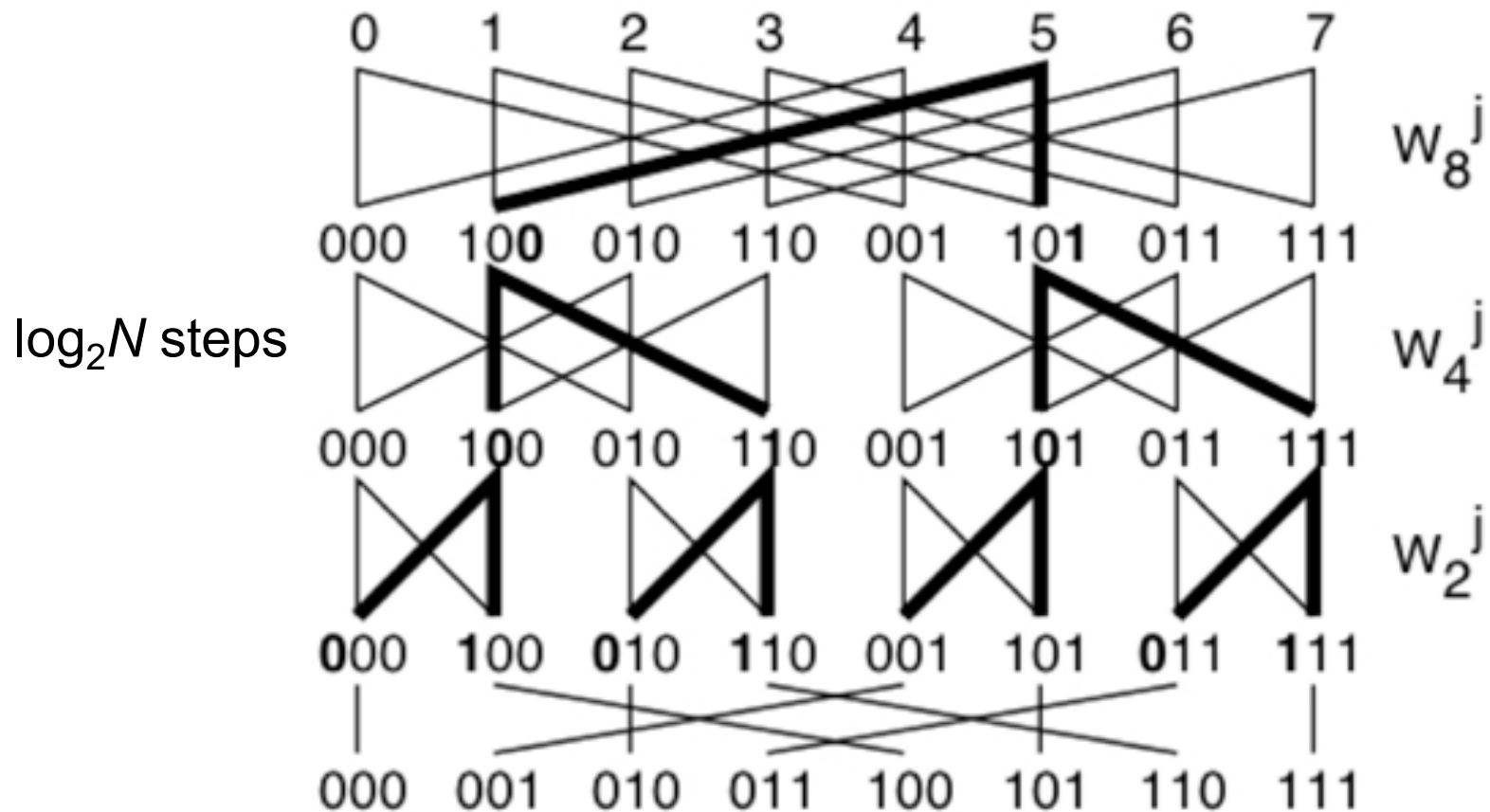


$$x_j = \frac{jL}{N}; \quad k_n = \frac{2\pi n}{L}$$

Numerics: Fast Fourier Transform

- $O(N \log N)$ fast Fourier-transform (FFT) algorithm is typically used to perform Fourier transform

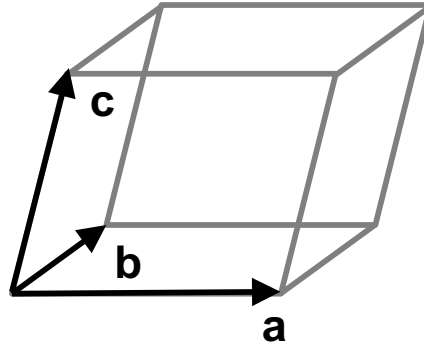
$$\psi(x_j) = \sum_{k_n} \psi_{k_n} \exp(ik_n x_j)$$



Butterfly (hypercube) data-exchange network

Periodic Solid

- Consider a periodic solid with the unit cell spanned by vectors \mathbf{a} , \mathbf{b} & \mathbf{c}



- Fourier transform of a periodic function

$$u(\mathbf{r}) = \sum_{\mathbf{G}} u_{\mathbf{G}} \exp(i\mathbf{G} \cdot \mathbf{r})$$

$$\mathbf{G} = \frac{2\pi}{\mathbf{a} \cdot (\mathbf{b} \times \mathbf{c})} [l(\mathbf{b} \times \mathbf{c}), m(\mathbf{c} \times \mathbf{a}), n(\mathbf{a} \times \mathbf{b})] \quad (l, m, n \in \mathbb{Z})$$

- Bloch's theorem

$$\begin{aligned} \psi_{n\mathbf{k}}(\mathbf{r}) &= \exp(i\mathbf{k} \cdot \mathbf{r}) u_{n,\mathbf{k}}(\mathbf{r}) \\ &= \sum_{\mathbf{G}} u_{n,\mathbf{k}}(\mathbf{G}) \exp(i(\mathbf{k} + \mathbf{G}) \cdot \mathbf{r}) \end{aligned}$$

band index

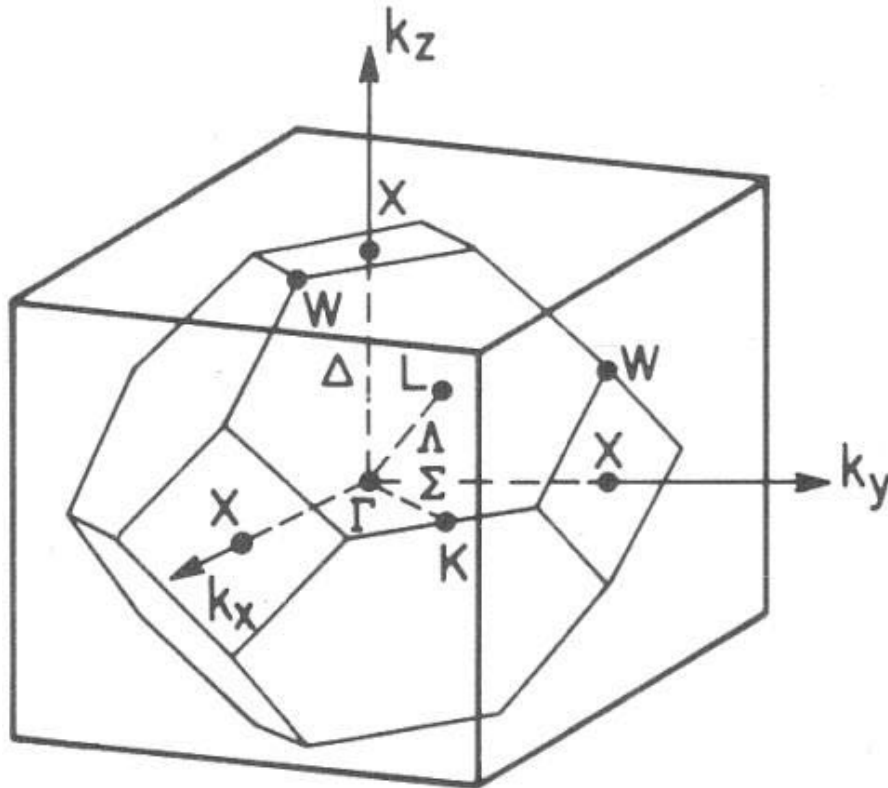
$\mathbf{k} \in$ first Brillouin zone in the reciprocal space

Electronic Bands: Infinite Lattice

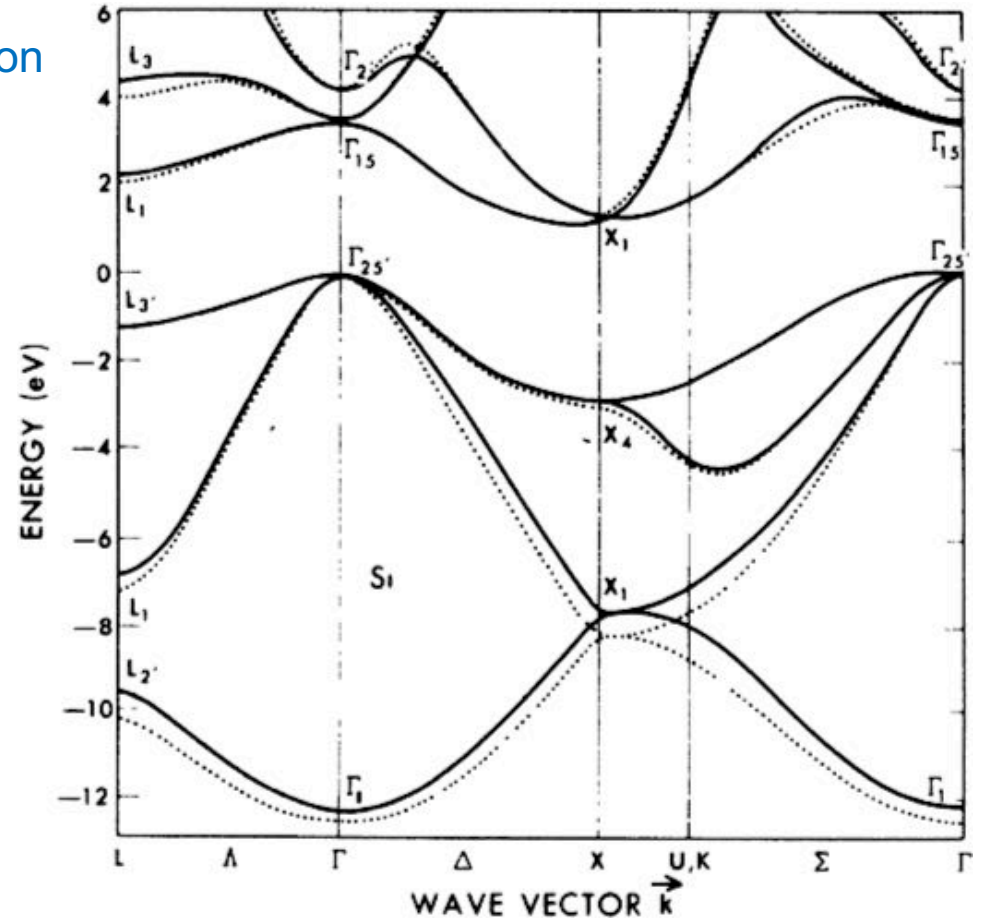
- **Bloch theorem:** $\psi_{n\mathbf{k}}(\mathbf{r}) = \exp(i\mathbf{k} \cdot \mathbf{r})u_{n,\mathbf{k}}(\mathbf{r})$

band index

periodic function



Brillouin zone of Si crystal



Kohn-Sham energy

J. R. Chelikowsky & M. L. Cohen, *Phys. Rev. B* 10, 5095 ('74)

Self-Consistent Field Iteration

$$\left(-\frac{\hbar^2}{2m} \frac{\partial^2}{\partial \mathbf{r}^2} + \hat{V}_{\text{ion}} + \hat{V}_{\text{H,xc}}[\rho(\mathbf{r})] \right) \psi_n(\mathbf{r}) = \epsilon_n \psi_n(\mathbf{r})$$

Given $\rho(\mathbf{r})$,
iteratively obtain
 $\{\psi_n, \epsilon_n\}$, e.g., by
preconditioned
conjugate gradient

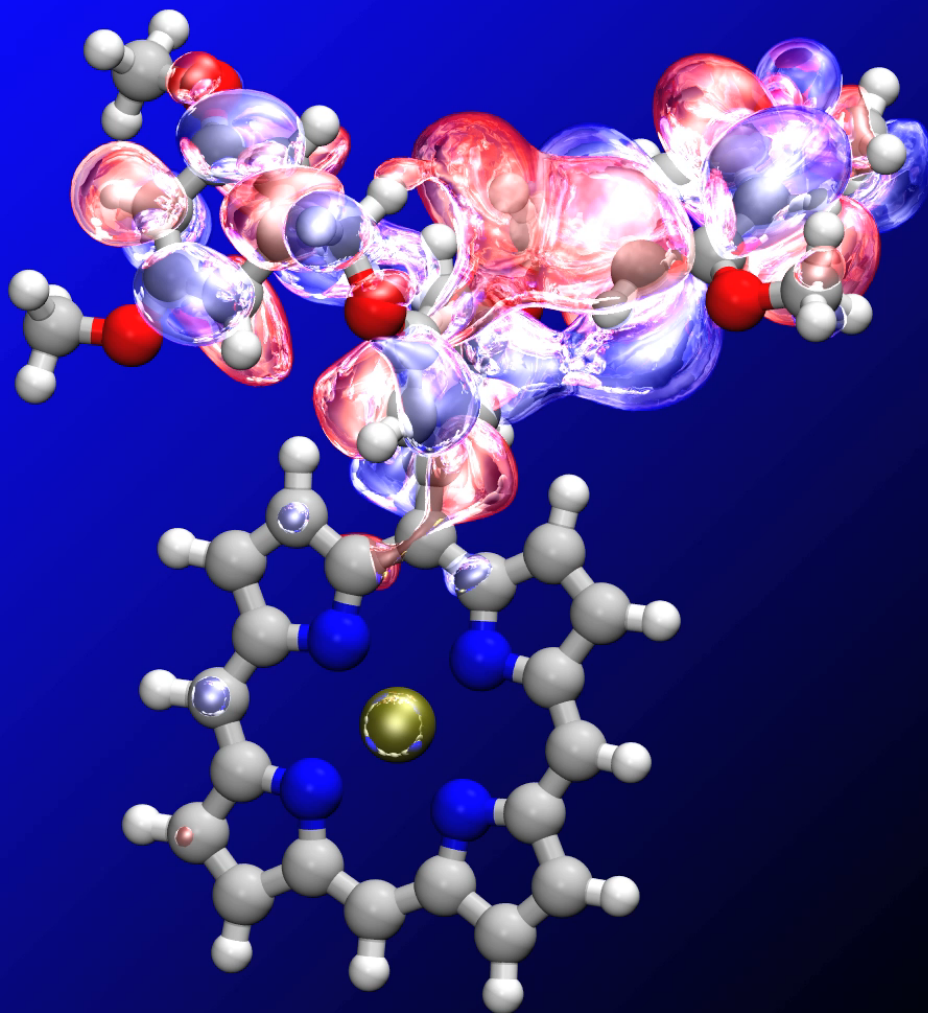
Given $\{\psi_n, \epsilon_n\}$,
determine μ and
compute $\rho(\mathbf{r})$

$$\rho(\mathbf{r}) = \sum_n |\psi_n(\mathbf{r})|^2 \Theta(\mu - \epsilon_n)$$

Chemical potential

$$N = \int d\mathbf{r} \rho(\mathbf{r})$$

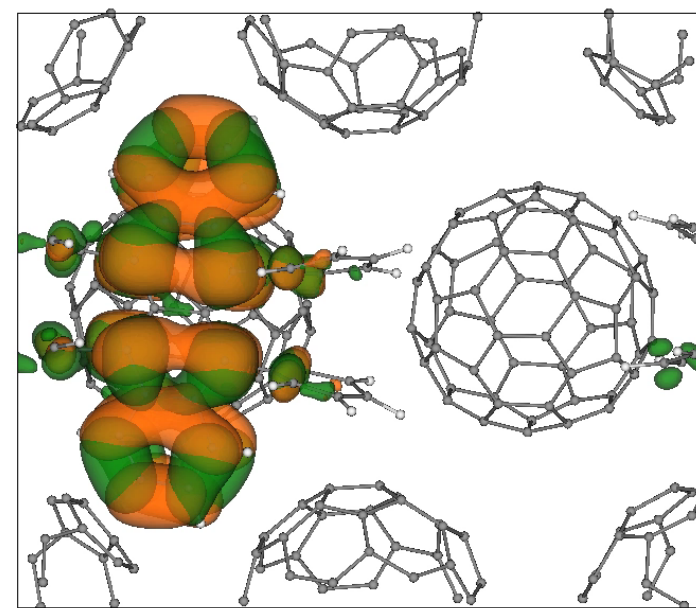
Nonadiabatic Quantum Molecular Dynamics



W. Mou *et al.*, *Appl. Phys. Lett.* **98**, 113301 ('11);
ibid. **100**, 203306 ('12); *J. Chem. Phys.* **136**,
184705 ('12); *Comput. Phys. Commun.* **184**, 1
('13); *Appl. Phys. Lett.* **102**, 093302 ('13); *ibid.*
102, 173301 ('13); *J. Chem. Phys.* **140**, 18A529
('14); *IEEE Computer* **48(11)**, 33 ('15); *Sci. Rep.* **5**,
19599 ('16); *Nature Commun.* **8**, 1745 ('17)

Zn porphyrin

Rubrene/C₆₀



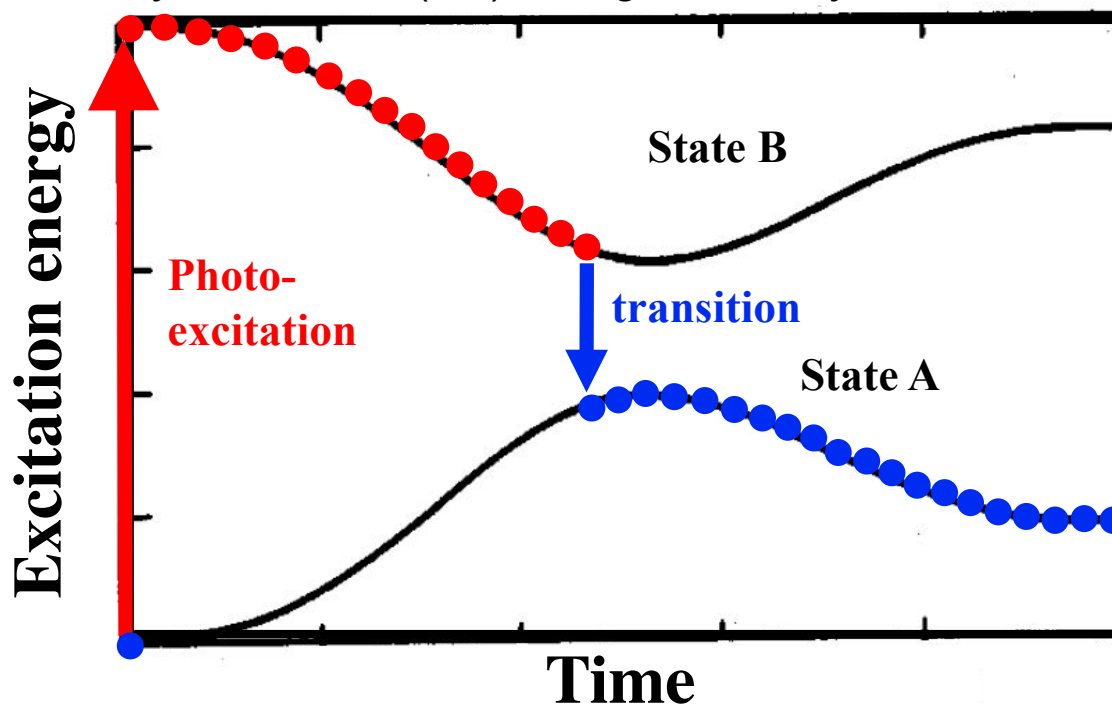
quasi-electron; quasi-hole

- **Excited states:** Linear-response time-dependent density functional theory [Casida, '95]
- **Interstate transitions:** Surface hopping [Tully, '90; Jaeger, Fisher & Prezhdo, '12]

TDDFT & Surface Hopping

- Incorporate electron transitions with the time-dependent density-functional theory (TDDFT) & surface-hopping method

Tully, *J. Chem. Phys.* **93**, 1061 ('90); Craig *et al.*, *Phys. Rev. Lett.* **95**, 163001 ('05)



- Electronic transitions from the current state to another occur stochastically based on the switching probability obtained by solving TDDFT equations

$$\Psi(\mathbf{r}, t) = \sum_J C_J^{(I)}(t) \Phi_J(\mathbf{r}; \mathbf{R}(t)) \quad C_J^{(I)}(0) = \delta_{I,J}$$

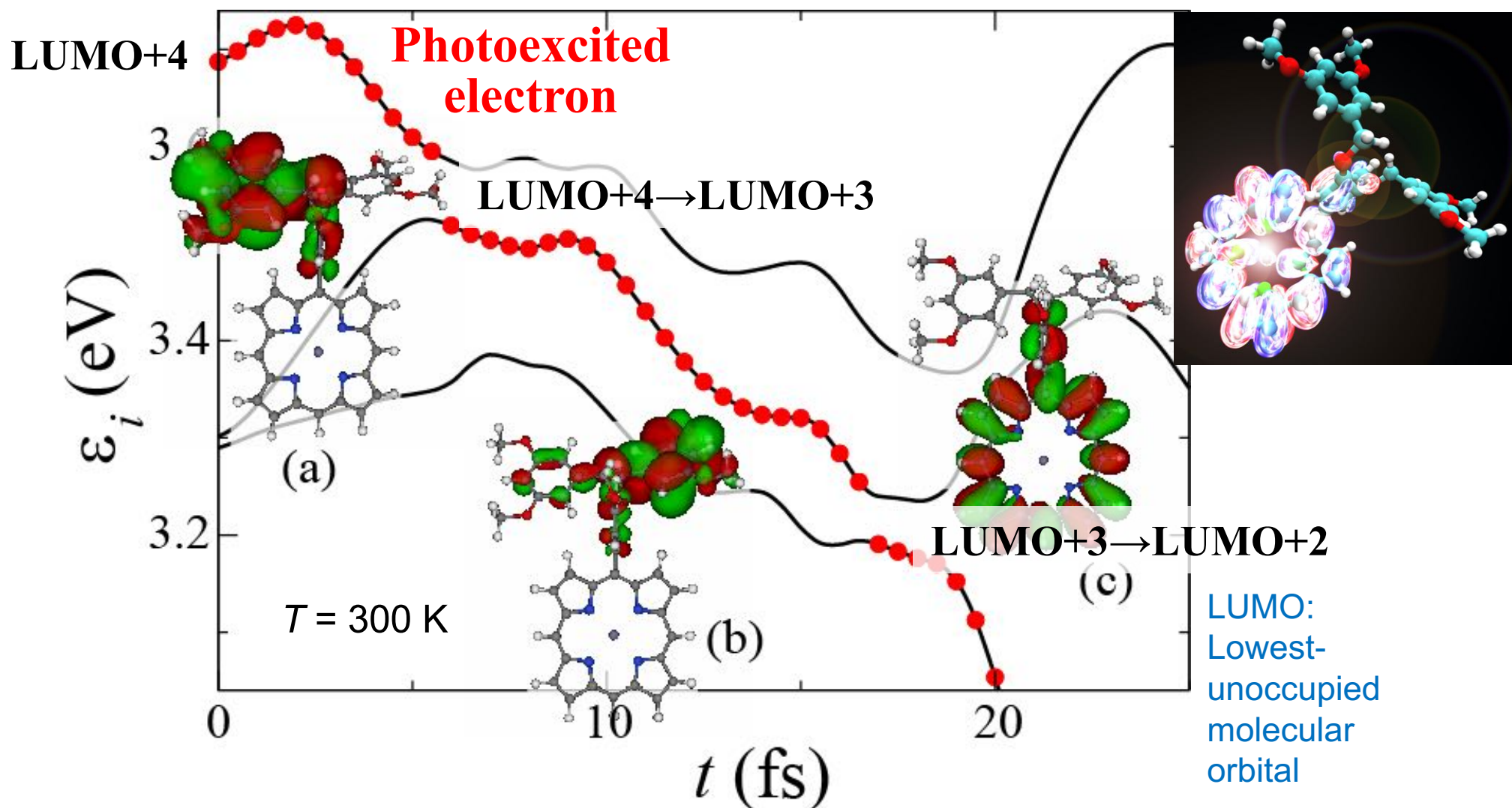
J-th adiabatic excited state

$$\frac{d}{dt} C_J^{(I)}(t) = - \sum_k C_k^{(I)}(t) \left(i\omega_K \delta_{JK} + \langle \Phi_J | \frac{\partial}{\partial t} | \Phi_K \rangle \right)$$

K-th excitation frequency

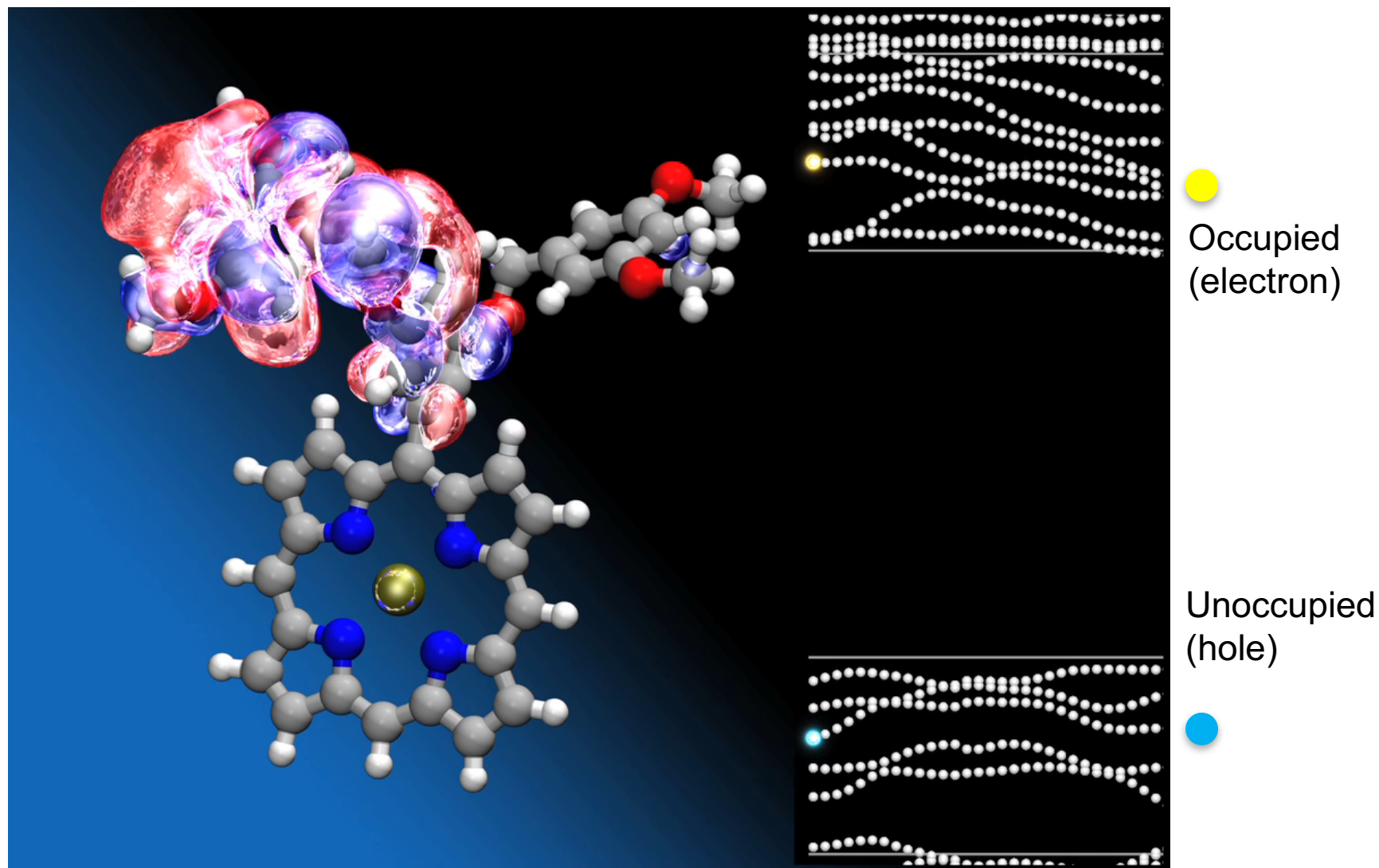
Nonadiabatic coupling

Example: Electron Transfer in a Dendrimer



- The photoexcited electron at the peripheral antenna is transferred to the core due to the energy-crossing & overlapping of orbitals assisted by thermal molecular motions

Electron Transfer in a Light-Harvesting Dendrimer



- The photoexcited electron at the peripheral antenna is transferred to the core due to the energy-crossing & overlapping of orbitals assisted by thermal molecular motions

Excitonic Effects: LR-TDDFT

- Excited electron-hole pairs within the linear-response time-dependent density functional theory (LR-TDDFT) [Casida, '95]

$$\delta V(t) = \delta v_{kl\tau}(t) \hat{a}_{k\tau}^+ \hat{a}_{l\tau} \longrightarrow \delta P_{ij\sigma}(t) = \delta \langle \Phi(t) | \hat{a}_{i\sigma}^+ \hat{a}_{j\sigma} | \Phi(t) \rangle$$

$\chi_{ij\sigma,kl\tau}(t-t') = \delta P_{ij\sigma}(t) / \delta v_{kl\tau}(t')$
electron
hole

- Excitation energies from the poles of the response function $\chi_{ij\tau,kl\sigma}(\omega)$

$2N_{\text{unoccupied}} N_{\text{occupied}} \times 2N_{\text{unoccupied}} N_{\text{occupied}}$ matrix eigenequation

$$\begin{pmatrix} \mathbf{A} & \mathbf{B} \\ \mathbf{B}^* & \mathbf{A}^* \end{pmatrix} \begin{pmatrix} \mathbf{X}_I \\ \mathbf{Y}_I \end{pmatrix} = \hbar\omega_I \begin{pmatrix} \mathbf{1} & \mathbf{0} \\ \mathbf{0} & -\mathbf{1} \end{pmatrix} \begin{pmatrix} \mathbf{X}_I \\ \mathbf{Y}_I \end{pmatrix}$$

I -th excitation energy

Kohn-Sham energy

$$A_{ia\sigma,jb\tau} = \delta_{\sigma,\tau} \delta_{i,j} \delta_{a,b} (\varepsilon_{a\sigma} - \varepsilon_{i\sigma}) + K_{ia\sigma,jb\tau} \quad B_{ia\sigma,jb\tau} = K_{ia\sigma,bj\tau}$$

$$K_{ia\sigma,i'a'\sigma'} = \iint \psi_{i\sigma}^*(\mathbf{r}) \psi_{a\sigma}(\mathbf{r}) \left(\frac{e^2}{|\mathbf{r}-\mathbf{r}'|} + \frac{\delta^2 E_{\text{xc}}}{\delta\rho_{\sigma}(\mathbf{r})\delta\rho_{\sigma'}(\mathbf{r}')} \right) \psi_{i'\sigma'}(\mathbf{r}') \psi_{a'\sigma'}^*(\mathbf{r}') d\mathbf{r} d\mathbf{r}'$$

Coulomb & exchange-correlation interaction matrix elements

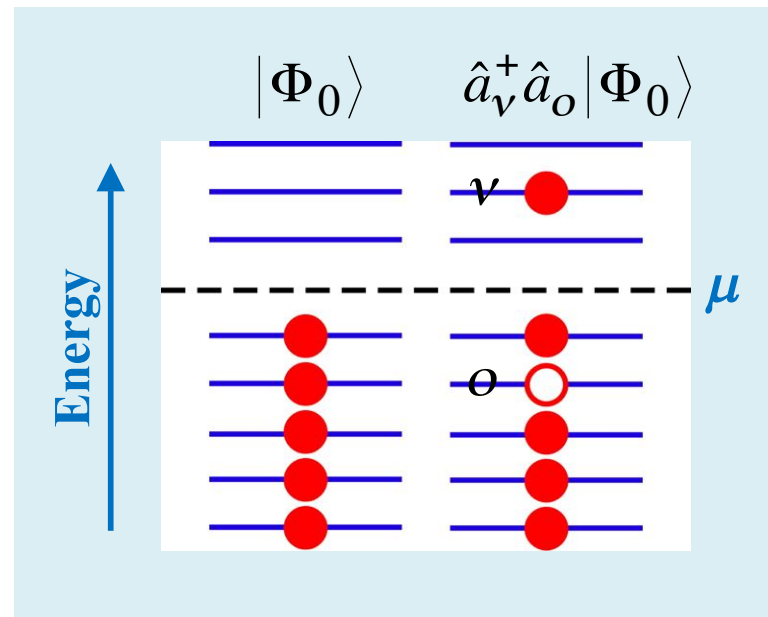
Electronic Excited States

- I -th excited state

$$|\Phi_I(\mathbf{r}; \mathbf{R})\rangle = \sum_{i \in \{\text{occupied}\}} \sum_{a \in \{\text{unoccupied}\}} \sum_{\sigma} \sqrt{\frac{\epsilon_{a\sigma} - \epsilon_{i\sigma}}{\hbar\omega_I}} (X_{I,ia\sigma} + Y_{I,ia\sigma}) \hat{a}_{a\sigma}^+ \hat{a}_{i\sigma} |\Phi_0(\mathbf{r}; \mathbf{R})\rangle$$

electron-hole pair

ground state



QXMD Code

- **Quantum molecular dynamics (QMD) code developed by Prof. Fuyuki Shimojo at Kumamoto University in Japan**
- **Various eXtensions co-developed with USC-CACS: Nonadiabatic QMD, linear-scaling divide-&-conquer, parallelization, *etc.***
- **Unique features:**
 - > **Interatomic forces with electronic excitation to study photo-excited lattice dynamics**
Shimojo *et al.*, *Comput. Phys. Commun.* **184**, 1 ('13)
 - > **Range-separated hybrid exact-exchange functional for exciton binding**
Tawada *et al.*, *J. Chem. Phys.* **120**, 8425 ('04)
 - > **Lean divide-&-conquer density functional theory (LDF-DFT) with small $O(N)$ prefactor**
Shimojo *et al.*, *J. Chem. Phys.* **140**, 18A529 ('14)
 - > **Omni-directional multiscale shock technique (OD-MSST)**
Shimamura *et al.*, *Appl. Phys. Lett.* **107**, 231903 ('15); **108**, 071901 ('16)
 - > **Berry-phase computation of bulk polarization**
- **Other features:**
 - > **Various functionals: spin-polarized, GGA+U, DFT+D, nonlocal correlation**
 - > **Nudged elastic band (NEB) method for energy-barrier calculation**

GitHub repository:

https://github.com/USCCACS/QXMD_Course

Software download site:

<https://magics.usc.edu/qxmd>

Current & Future Computing Platforms

- Won two DOE supercomputing awards to develop & deploy metascalable (“design once, scale on future platforms”) simulation algorithms (2017-2020)



- NAQMD & RMD simulations on full 800K cores

Innovative & Novel Computational Impact on Theory & Experiment

Title: “Petascale Simulations for Layered Materials Genome”

Principal Investigator:

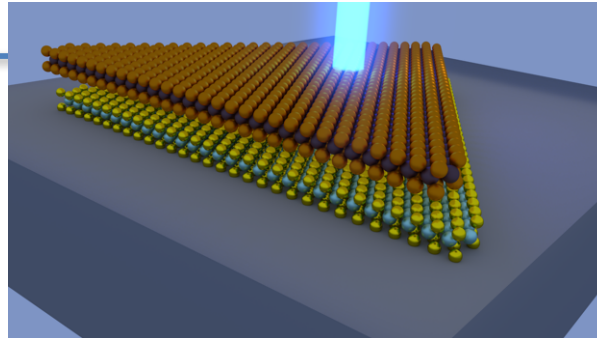
Aiichiro Nakano, University of Southern California

Co-Investigator:

Priya Vashishta, University of Southern California



786,432-core IBM Blue Gene/Q

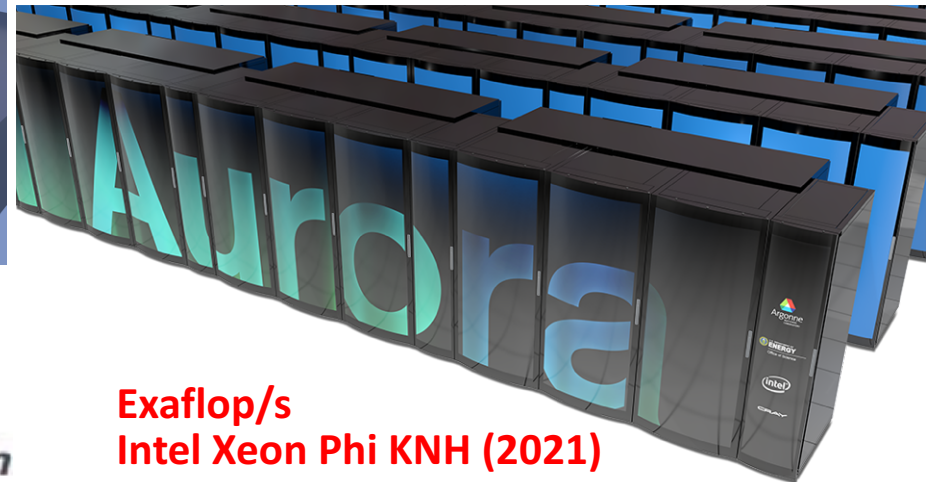


Early Science Projects for Aurora

Supercomputer Announced

Metascalable layered materials genome

Investigator: Aiichiro Nakano, University of Southern California



Exaflop/s
Intel Xeon Phi KNH (2021)

- One of 10 exclusive users of the next-generation DOE supercomputer

But...



Intel Dumps Knights Hill, Future of Xeon Phi Product Line Uncertain

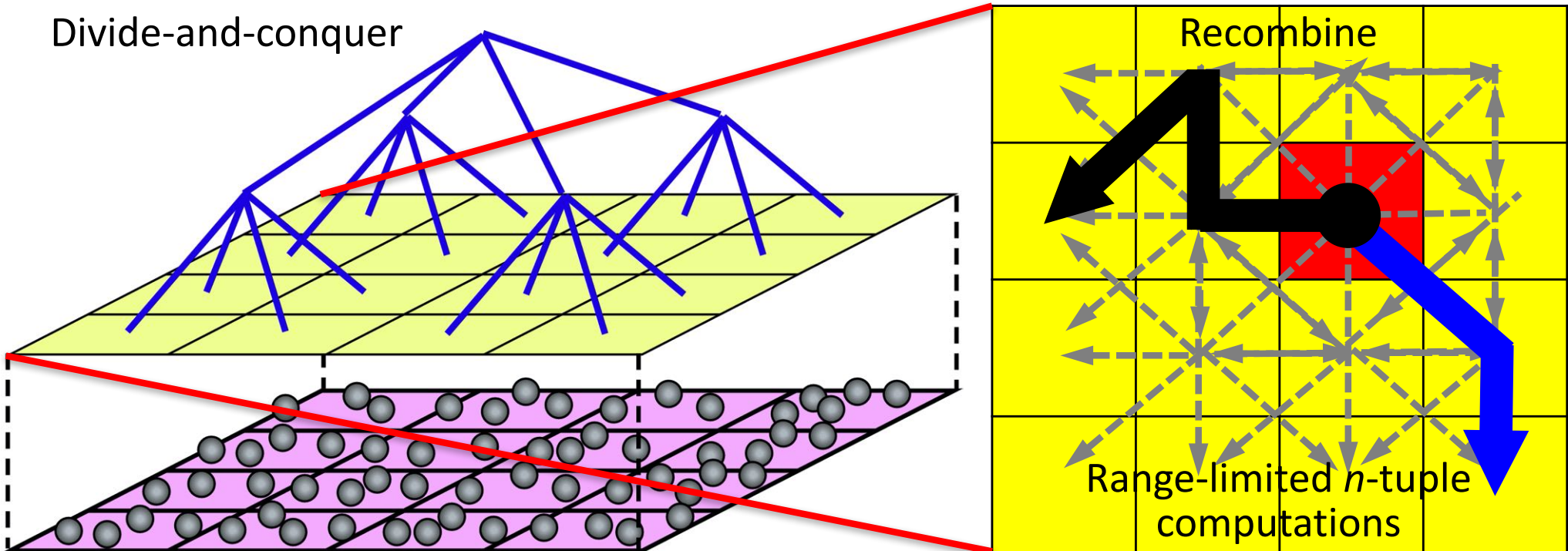
Michael Feldman | November 15, 2017 04:34 CET

<https://www.top500.org/news/>

- Need *metascalable* (or “design once, scale on new architectures”) parallel applications
- Proposed *divide-conquer-recombine*

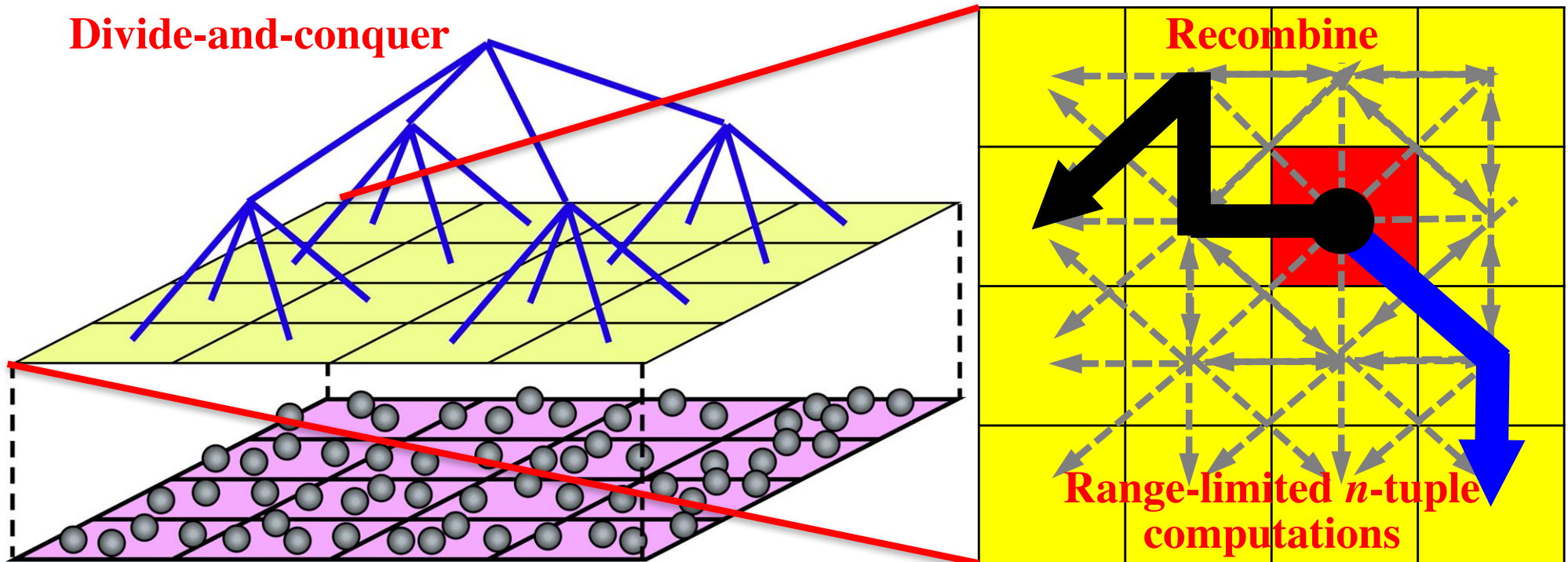
F. Shimojo *et al.*, *J. Chem. Phys.* **140**, 18A529 ('14);
K. Nomura *et al.*, *ACM/IEEE SC14* ('14)

Divide-and-conquer



M. Kunaseth *et al.*, *ACM/IEEE SC13* ('13)

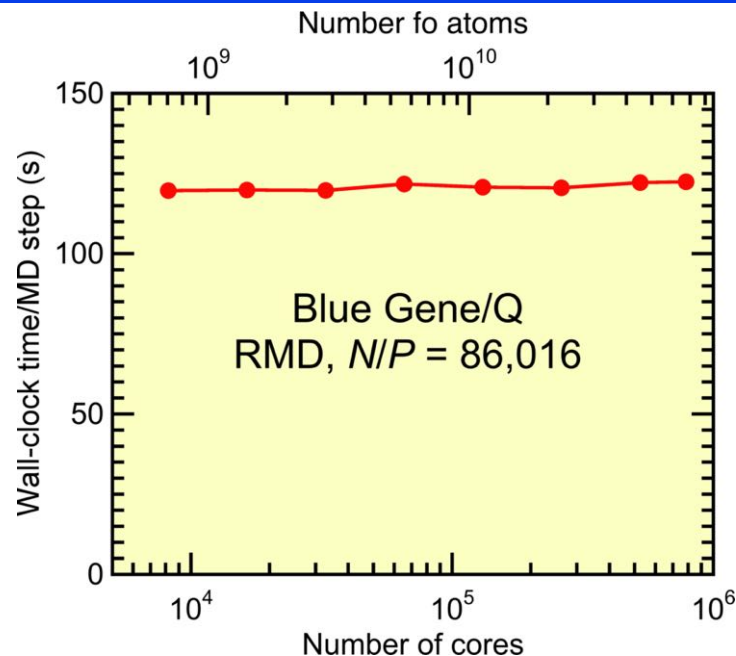
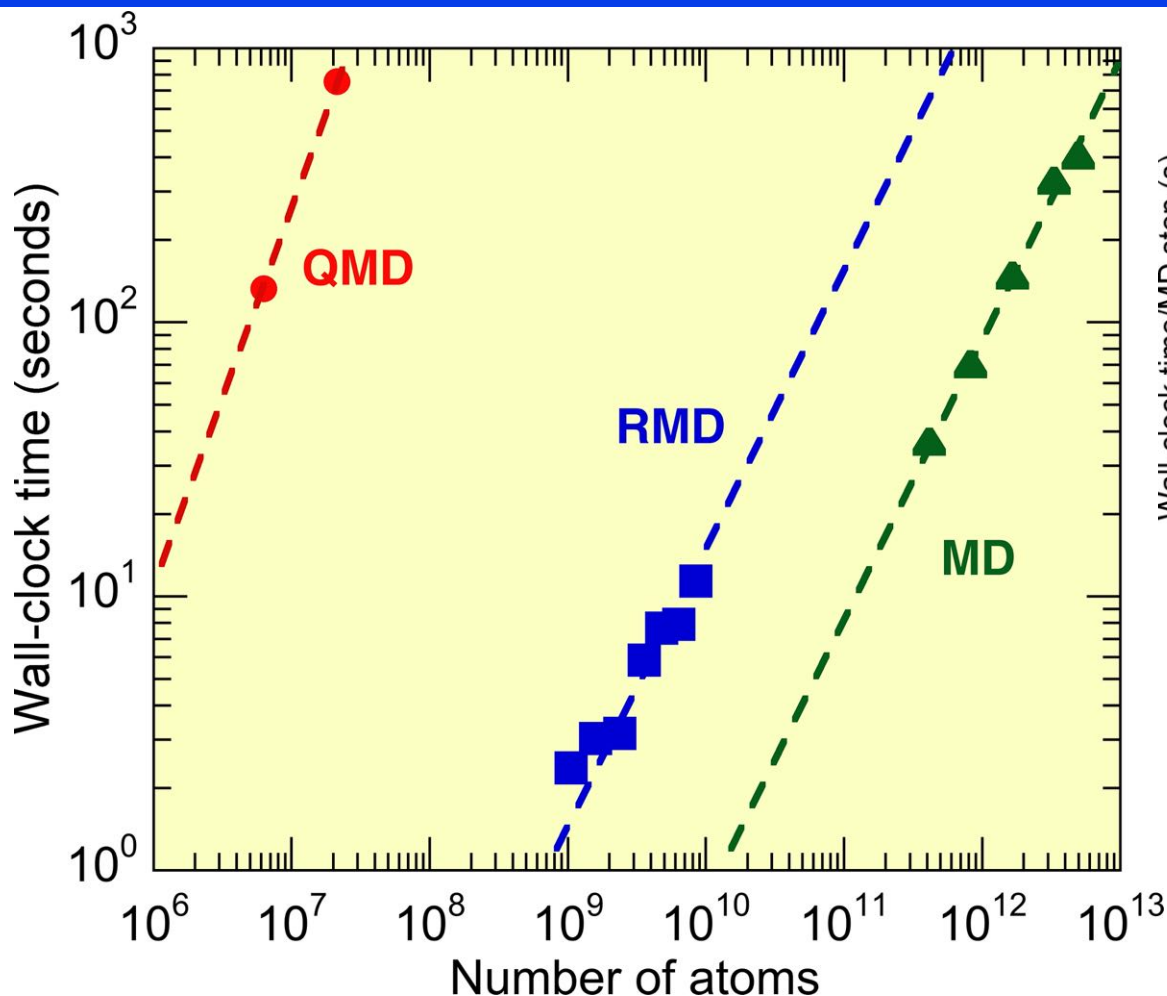
Divide-Conquer-Recombine (DCR) Engines



M. Kunaseth et al., ACM/IEEE SC13

- **Quantum MD:** Lean divide-&-conquer density functional theory (LDC-DFT) algorithm minimizes the prefactor of $O(N)$ computational cost
F. Shimojo et al., *J. Chem. Phys.* **140**, 18A529 ('14); K. Nomura et al., *IEEE/ACM SC14*
- **Reactive MD:** Extended-Lagrangian reactive molecular dynamics (XRMD) algorithm eliminates the speed-limiting charge iteration
K. Nomura et al., *Comput. Phys. Commun.* **192**, 91 ('15)

Scalable Simulation Algorithm Suite



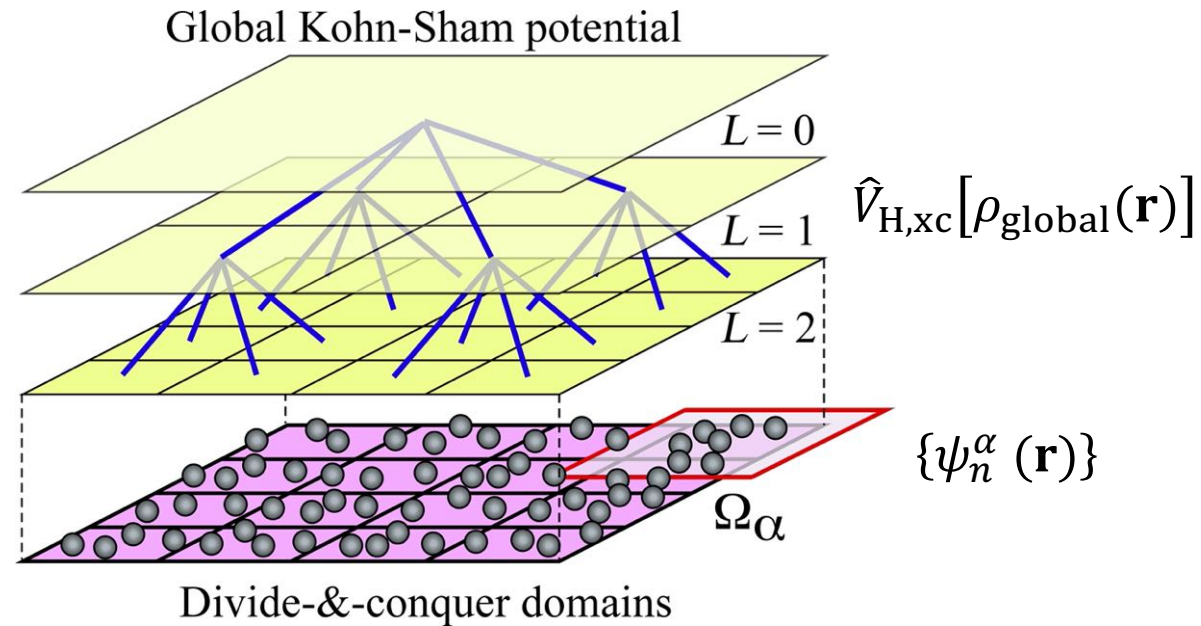
QMD (quantum molecular dynamics): DC-DFT

RMD (reactive molecular dynamics): F-ReaxFF

MD (molecular dynamics): MRMD

- **4.9 trillion-atom space-time multiresolution MD (MRMD) of SiO_2**
- **67.6 billion-atom fast reactive force-field (F-ReaxFF) RMD of RDX**
- **39.8 trillion grid points (50.3 million-atom) DC-DFT QMD of SiC**
parallel efficiency 0.984 on 786,432 Blue Gene/Q cores

Divide-&-Conquer Density Functional Theory



- **Overlapping spatial domains:** $\Omega = \cup_\alpha \Omega_\alpha$
- **Domain Kohn-Sham equations**

Global-local
self-consistent
field (SCF)
iteration

$$\left(-\frac{1}{2} \nabla^2 + \hat{V}_{\text{ion}} + \hat{V}_{H,xc}[\rho_{\text{global}}(\mathbf{r})] \right) \psi_n^\alpha(\mathbf{r}) = \epsilon_n^\alpha \psi_n^\alpha(\mathbf{r})$$

- **Global & domain electron densities**

$$\rho_{\text{global}}(\mathbf{r}) = \sum_\alpha p_\alpha(\mathbf{r}) \rho_\alpha(\mathbf{r}) \quad \leftarrow \quad \rho_\alpha(\mathbf{r}) = \sum_n [\psi_n^\alpha]^2 \Theta(\mu - \epsilon_n^\alpha)$$

Domain support function $\sum_\alpha p_\alpha(\mathbf{r}) = 1$

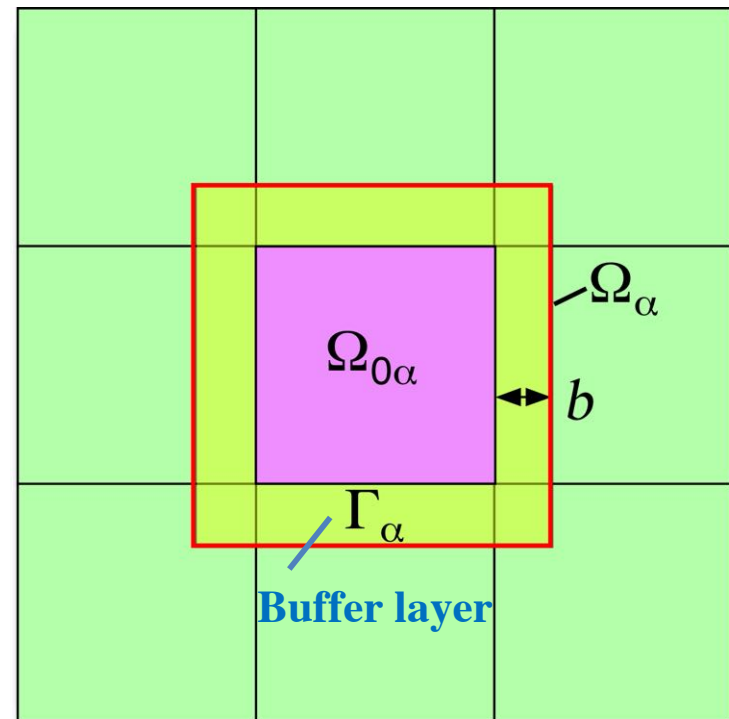
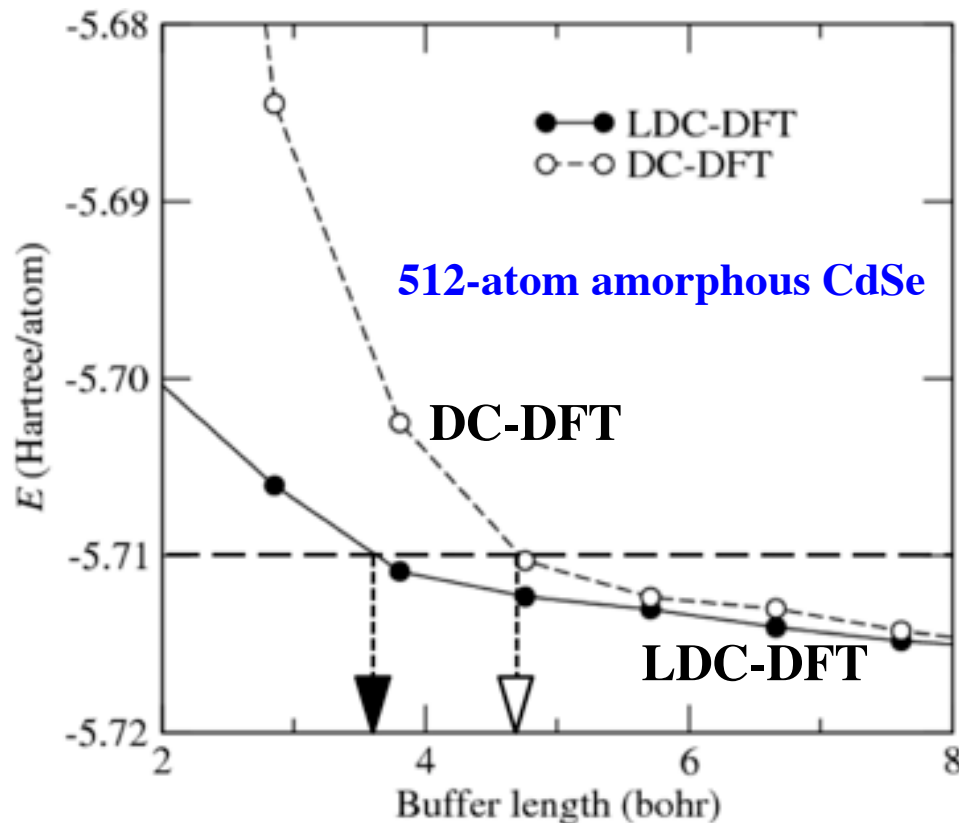
Global chemical potential $N = \int d\mathbf{r} \rho_{\text{global}}(\mathbf{r})$

Lean Divide-&-Conquer (LDC) DFT

- Density-adaptive boundary potential to reduce the $O(N)$ prefactor

$$v_{\alpha}^{bc}(\mathbf{r}) = \int d\mathbf{r}' \frac{\partial v(\mathbf{r})}{\partial \rho(\mathbf{r}')} (\rho_{\alpha}(\mathbf{r}) - \rho_{\text{global}}(\mathbf{r})) \cong \frac{\rho_{\alpha}(\mathbf{r}) - \rho_{\text{global}}(\mathbf{r})}{\xi}$$

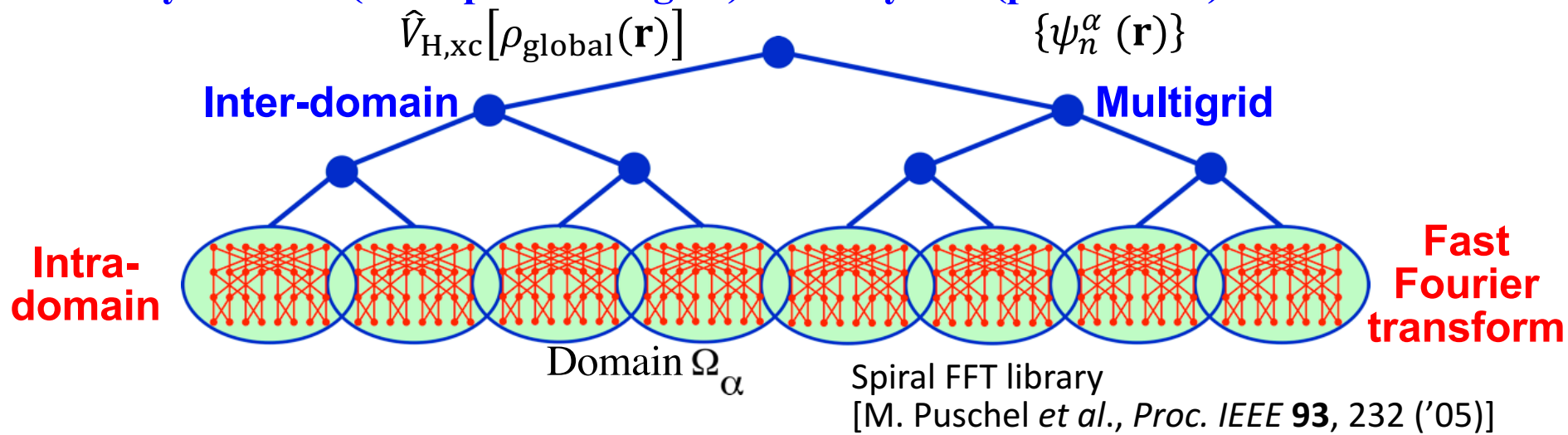
- More rapid energy convergence of LDC-DFT compared with nonadaptive DC-DFT



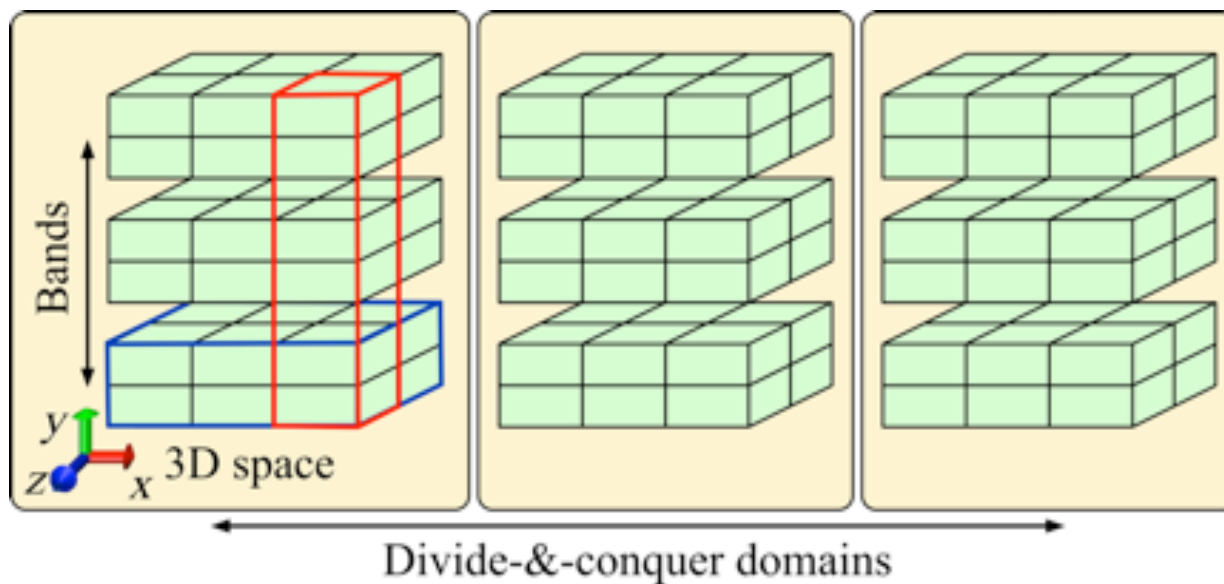
- Factor 2.03 (for $\nu = 2$) \sim 2.89 (for $\nu = 3$) reduction of the computational cost with an error tolerance of 5×10^{-3} a.u. (per-domain complexity: n^{ν})

Hierarchical Computing

- Globally scalable (real-space multigrid) + locally fast (plane wave) electronic solver

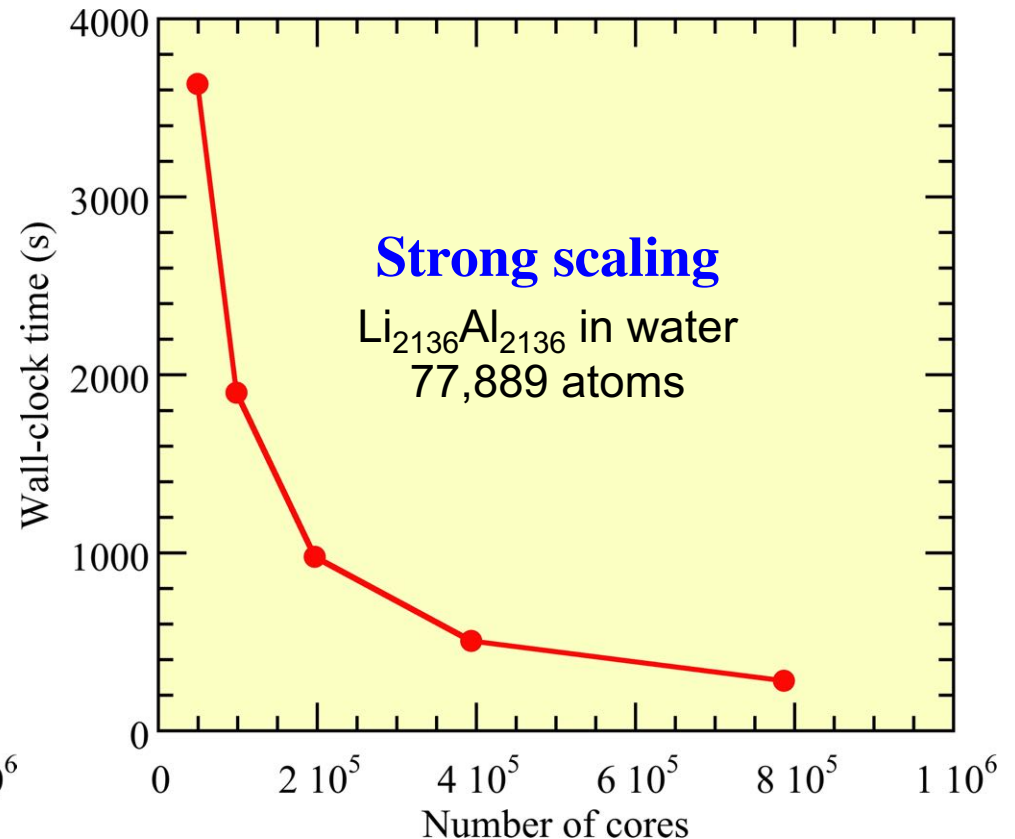
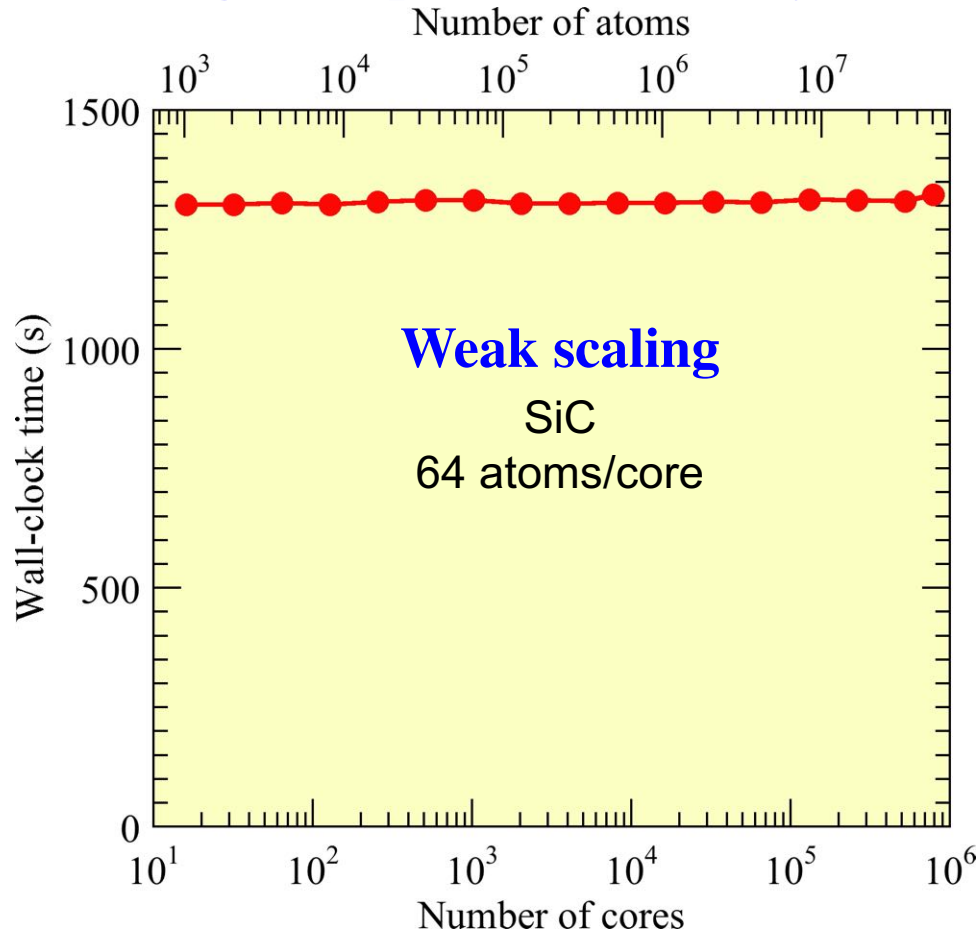


- Hierarchical band (*i.e.* Kohn-Sham orbital) + space + domain (BSD) decomposition



Parallel Performance

- **Weak-scaling parallel efficiency is 0.984 on 786,432 Blue Gene/Q cores for a 50,331,648-atom SiC system**
- **Strong-scale parallel efficiency is 0.803 on 786,432 Blue Gene/Q cores**



- **62-fold reduction of time-to-solution** [441 s/SCF-step for 50.3M atoms] **from the previous state-of-the-art** [55 s/SCF-step for 102K atoms, Osei-Kuffuor *et al.*, *PRL* '14]

K. Nomura *et al.*, *IEEE/ACM Supercomputing, SC14* ('14)

Floating Point Performance

- Transform from band-by-band to all-band computations to utilize a matrix-matrix subroutine (DGEMM) in the level 3 basic linear algebra subprograms (BLAS3) library
- Algebraic transformation of computations

Example: Nonlocal pseudopotential operation

D. Vanderbilt, *Phys. Rev. B* **41**, 7892 ('90)

$$\hat{v}_{\text{nl}}|\psi_n^\alpha\rangle = \sum_I^{N_{\text{atom}}} \sum_{ij}^{L_{\text{max}}} |\beta_{i,I}\rangle D_{ij,I} \langle \beta_{j,I} | \psi_n^\alpha \rangle \quad (n = 1, \dots, N_{\text{band}})$$

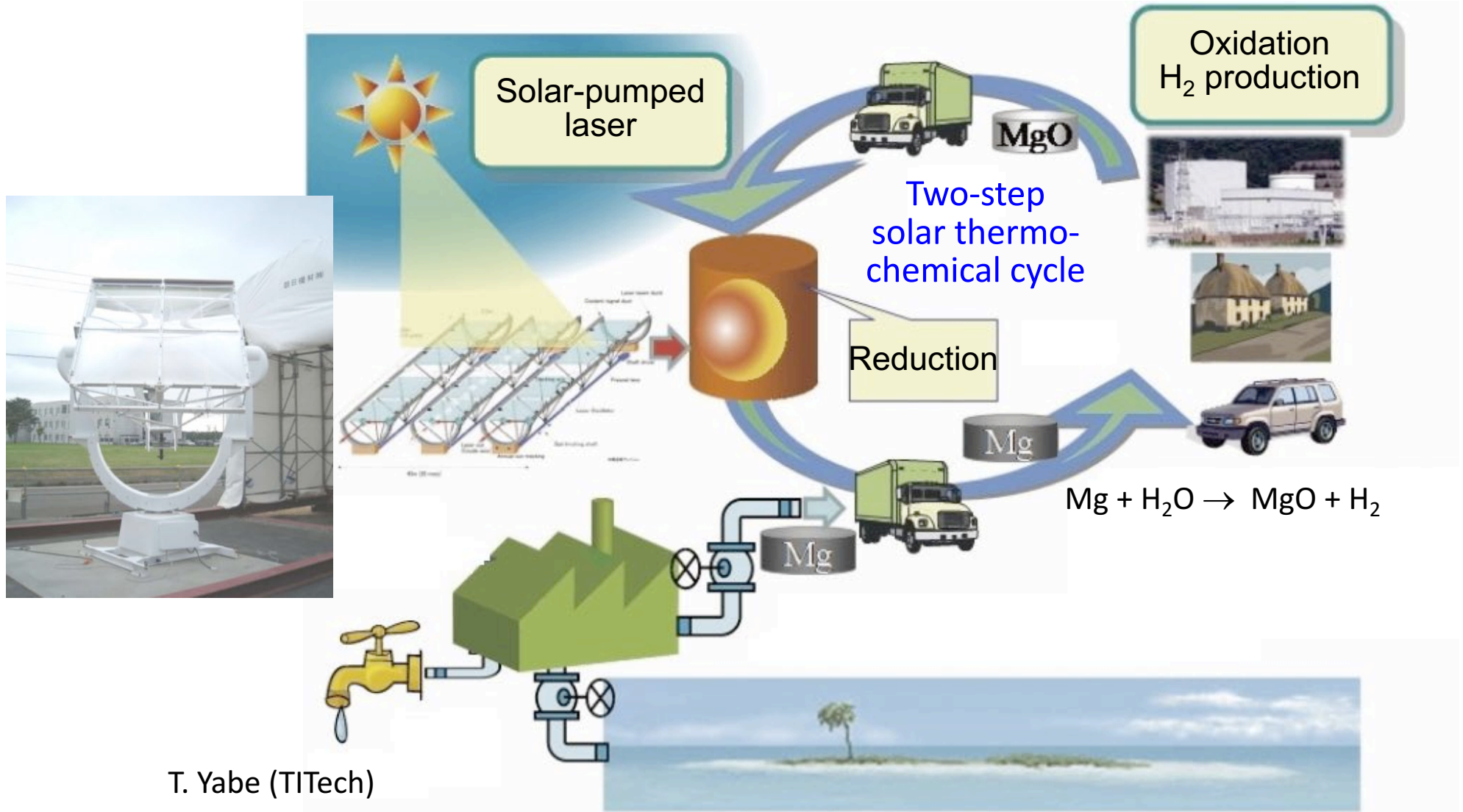


$$\Psi = [|\psi_1^\alpha\rangle, \dots, |\psi_{N_{\text{band}}}^\alpha\rangle] \quad \tilde{\mathbf{B}}(i) = [|\beta_{i,1}\rangle, \dots, |\beta_{i,N_{\text{atom}}}\rangle] \quad [\tilde{\mathbf{D}}(i,j)]_{I,J} = D_{ij,I} \delta_{IJ}$$

$$\hat{v}_{\text{nl}}\Psi = \sum_{i,j}^L \tilde{\mathbf{B}}(i) \tilde{\mathbf{D}}(i,j) \tilde{\mathbf{B}}(j)^T$$

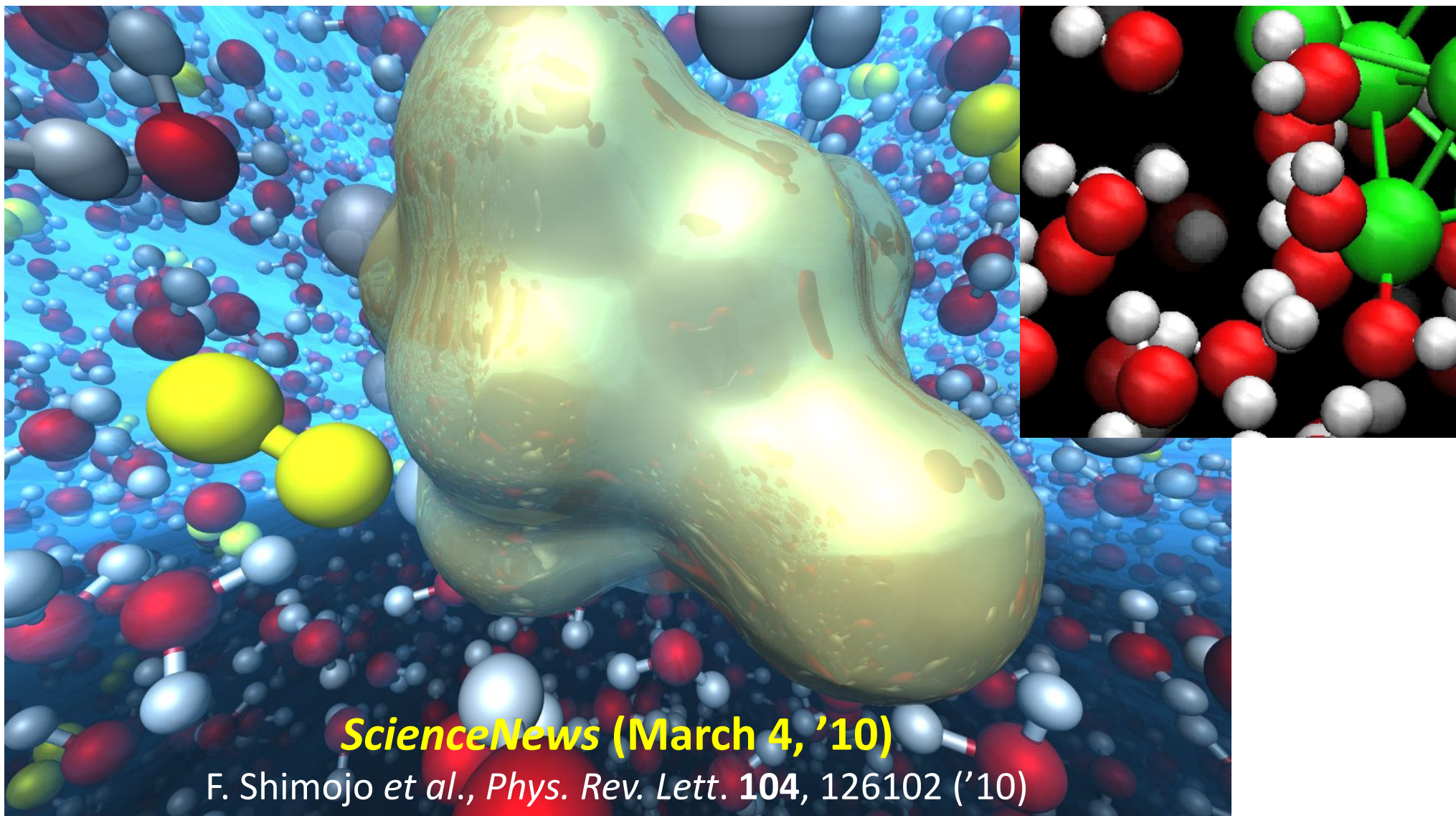
- **50.5%** of the theoretical peak FLOP/s performance on 786,432 Blue Gene/Q cores (entire Mira at the Argonne Leadership Computing Facility)
- **55%** of the theoretical peak FLOP/s on Intel Xeon E5-2665

Renewal Energy Cycle by Metal Carriers



- **Problem:** Accelerated hydrogen-production reaction kinetics for metal (Mg, Al, Zn, Fe) + water?

Nanotechnology Solution



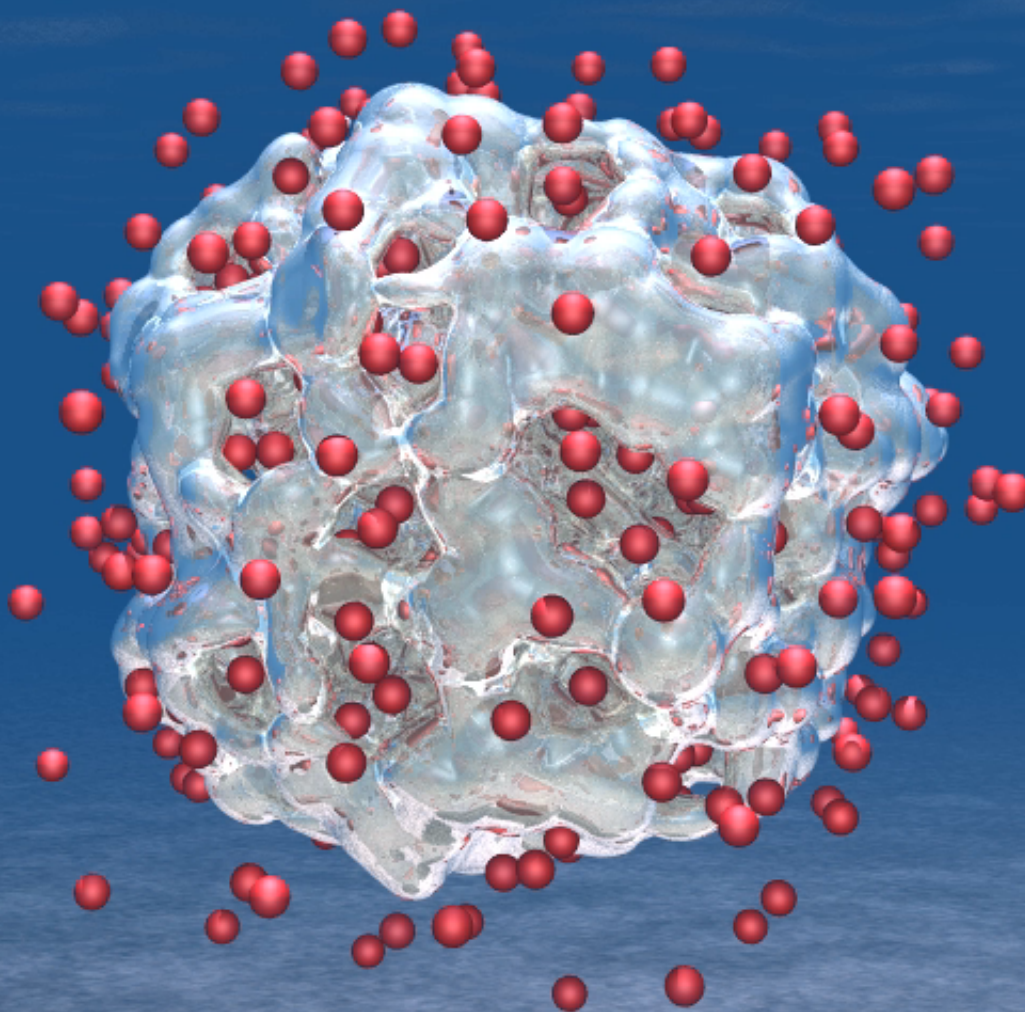
- **QMD simulation shows rapid H₂ production from water by a superatom* (Al₁₇), but the technology is not scalable to larger particle sizes**

*Roach, Castleman, Khanna *et al.*, *Science* **323**, 492 ('09)

H₂ Production from Water Using LiAl Particles

16,661-atom QMD simulation of Li₄₄₁Al₄₄₁ in water
on 786,432 IBM Blue Gene/Q cores

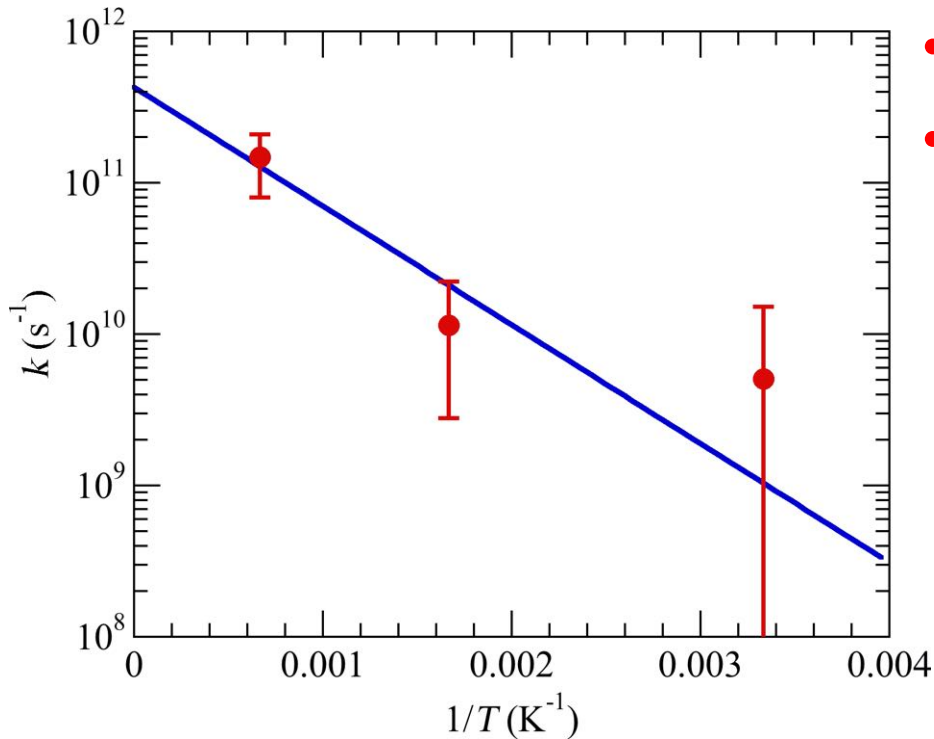
K. Shimamura *et al.*,
Nano Lett. **14**, 4090 ('14)



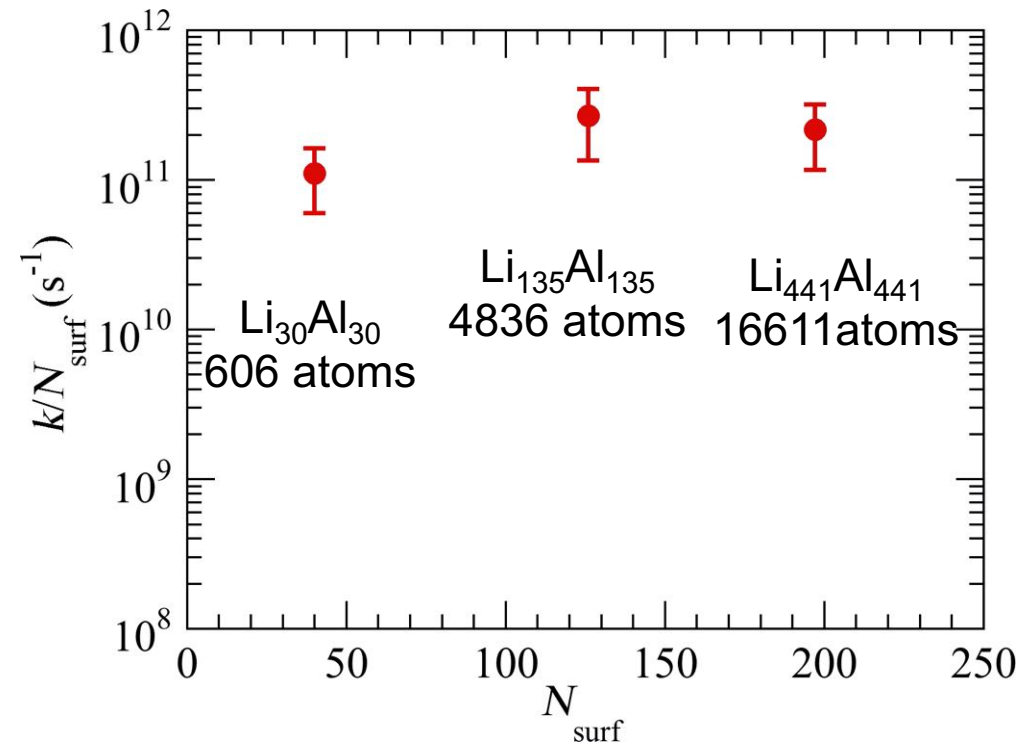
21,140 time steps (129,208 self-consistent-field iterations)

Rapid & Scalable H₂ Production

- Orders-of-magnitude faster H₂ production from water than with pure Al



- Activation barrier = 0.068 eV
- Reaction rate = 1.04 × 10⁹ (s⁻¹) per LiAl pair at 300 K

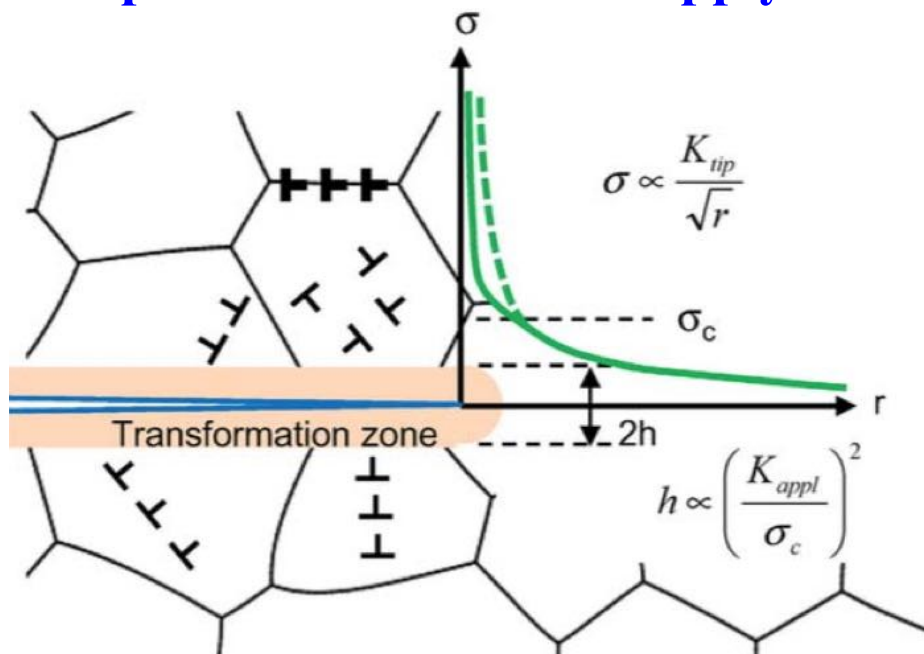
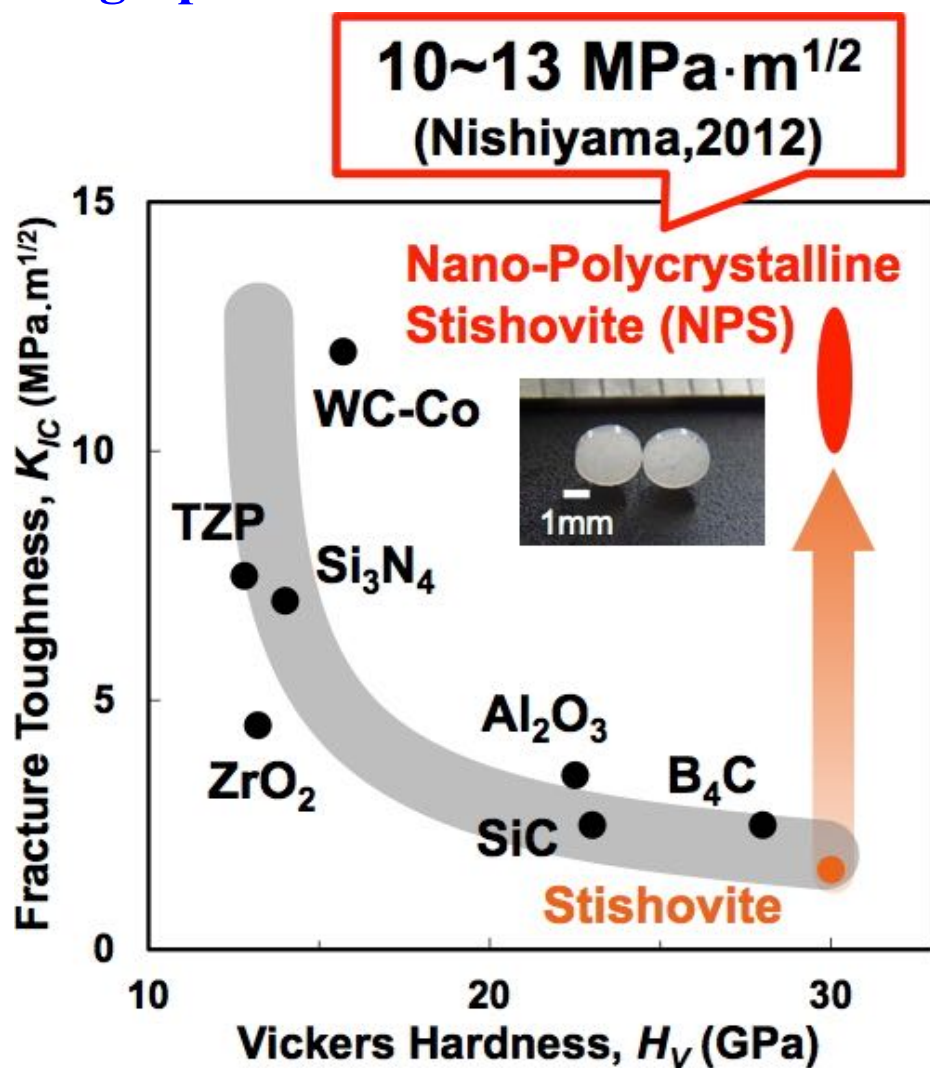


- Reaction rate does not decrease for larger particles → industrial scalability

K. Shimamura *et al.*, *Nano Lett.* **14**, 4090 ('14); K. Nomura *et al.*, *IEEE/ACM SC14* ('14)

Crack Self-Healing Stishovite

- Superhard, ultratough nano-polycrystalline stishovite (NPS) synthesized
N. Nishiyama *et al.*, *Scripta Mater.* **67**, 955 ('12); *Sci. Rep.* **4**, 6588 ('14)
- Made of Earth-abundant silica glass, NPS provides sustainable supply of high-performance ceramics

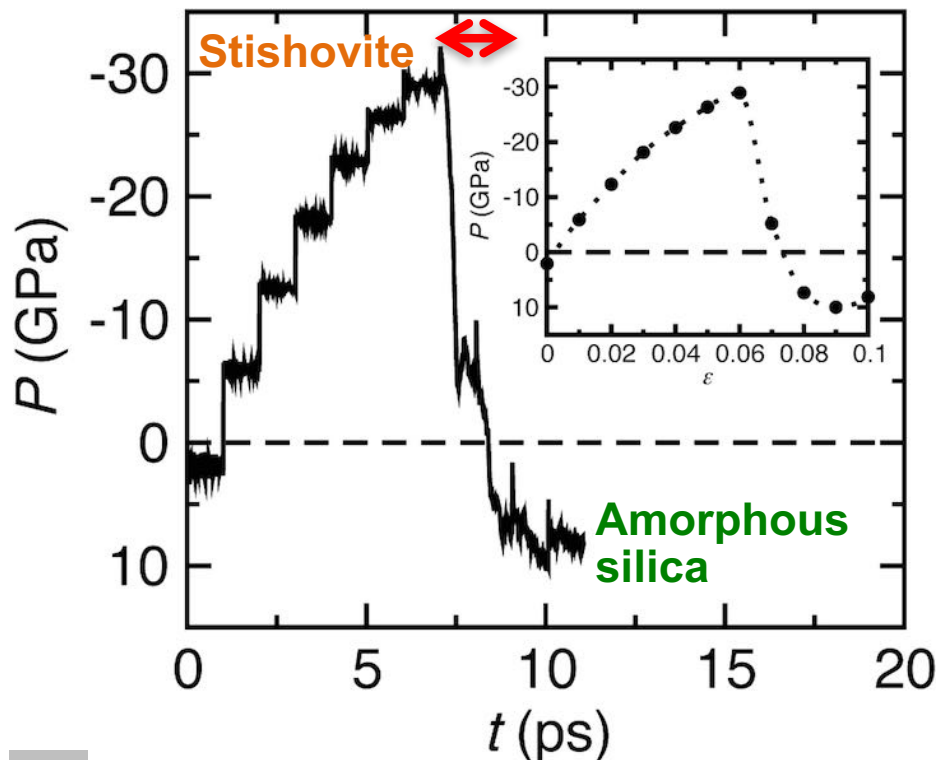
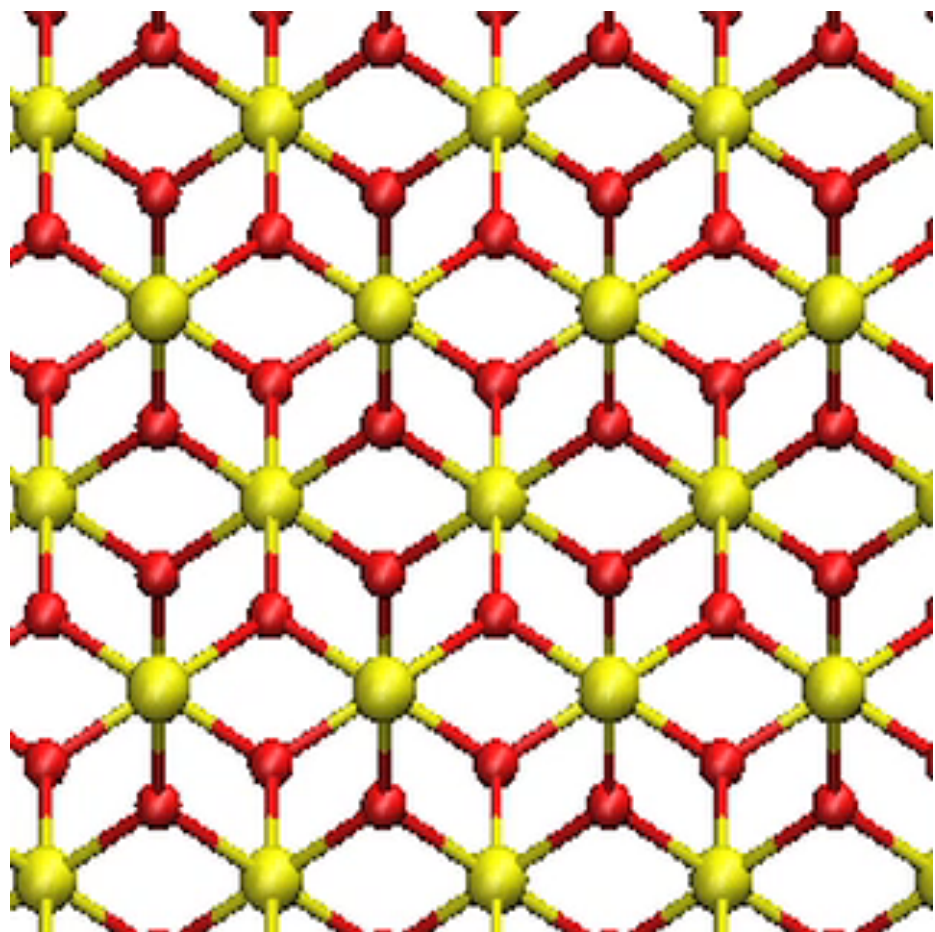


K. Yoshida *et al.*, *Sci. Rep.* **5**, 10993 ('15);
Acta Mater. **124**, 316 ('17)

- Toughening mechanism hypothesized to be amorphization under tension
- To catch up with a fast moving crack, amorphization needs rapid, but no theoretical nor experimental evidence

Rapid Tensile Amorphization

- QMD simulation reveals rapid amorphization of stishovite within picoseconds under tension ~ 30 GPa

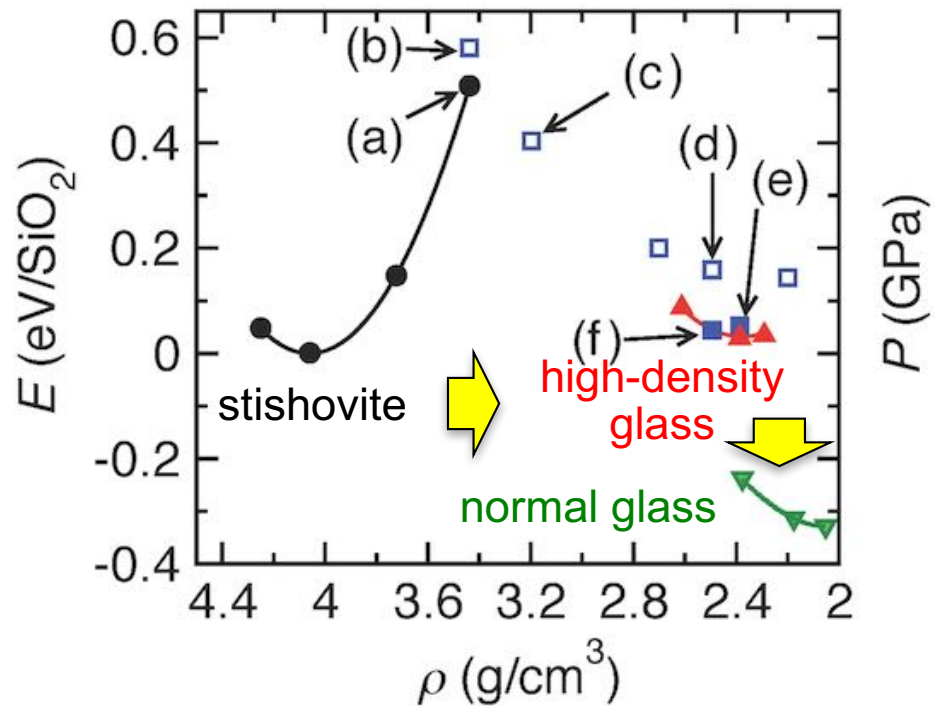
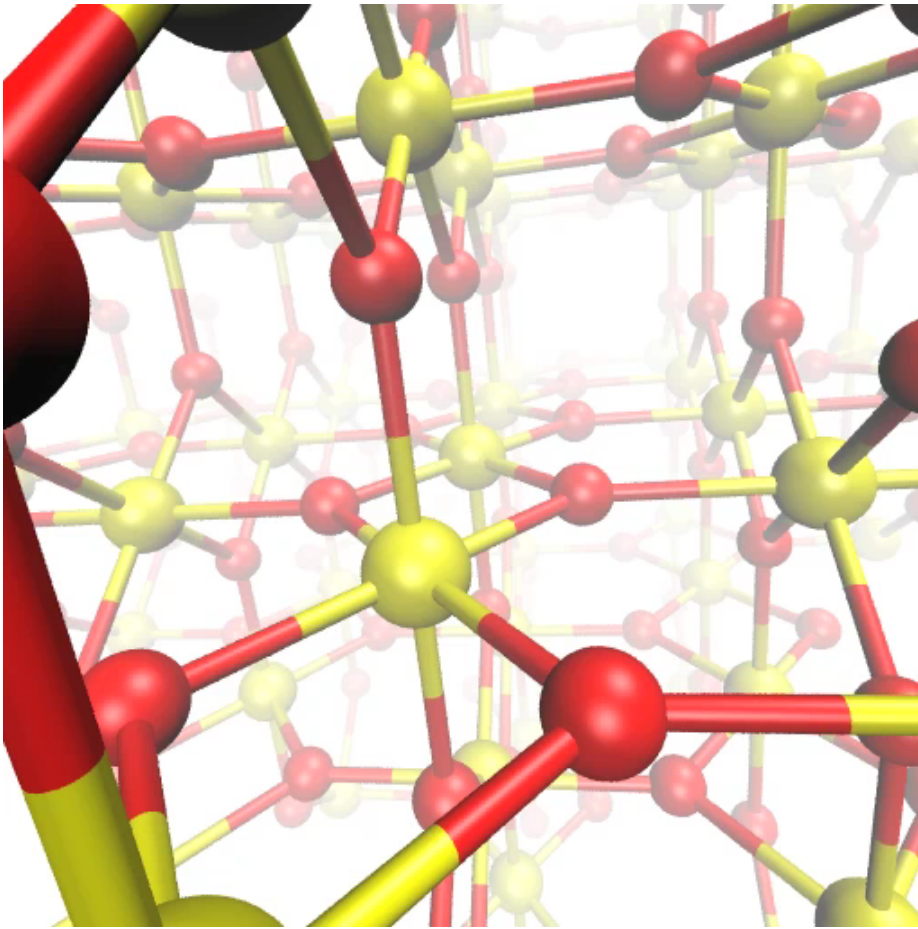


$$\text{Volume}_{\text{amorphous silica}} \sim 2 \times \text{Volume}_{\text{stishovite}}$$

- The rapid & expansive amorphization can catch up with, screen & self-heal a fast moving crack

Rapid Amorphization Mechanism

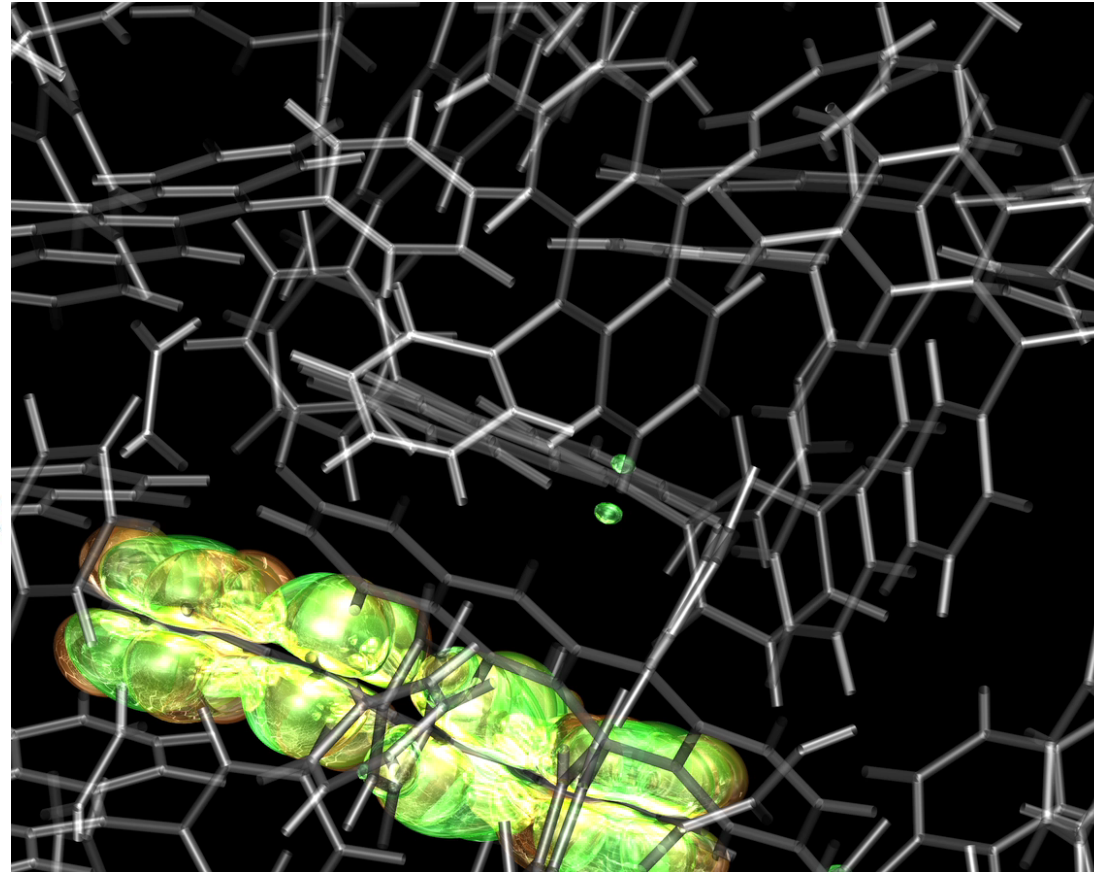
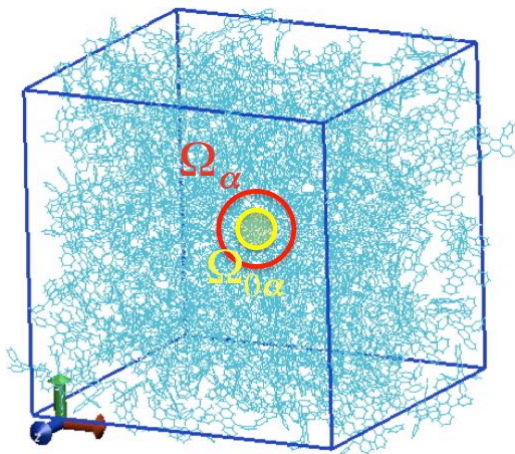
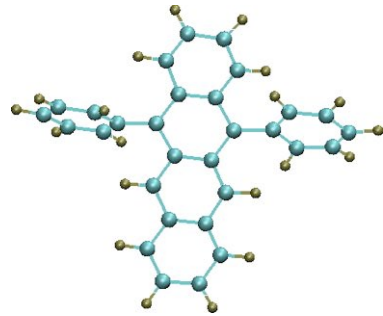
- Found a displacive amorphization mechanism that only involves short-distance collective motions of atoms, thereby facilitating the rapid transformation



- Two-step amorphization pathway from stishovite to glass involves an intermediate state akin to an experimentally suggested “high-density glass polymorph”

Singlet Fission in Amorphous DPT

- Photo-current doubling by splitting a singlet exciton into 2 triplet excitons
- Singlet fission in mass-produced disordered organic solid → efficient low-cost solar cells
- **Experimental breakthrough:** SF found in amorphous diphenyl tetracene (DPT)



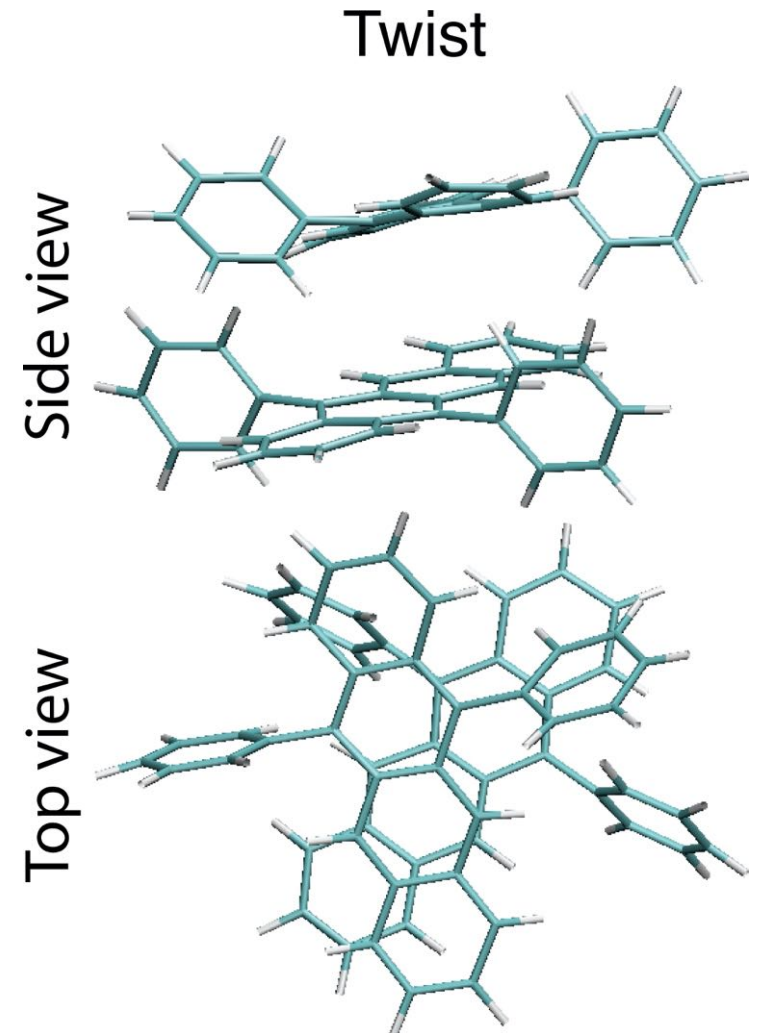
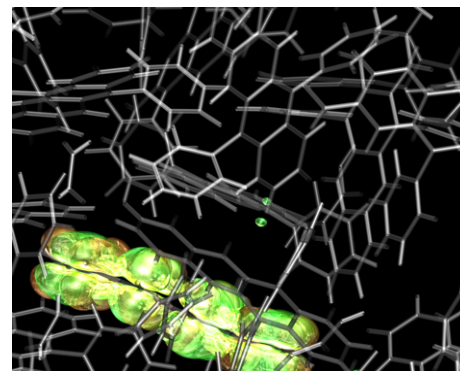
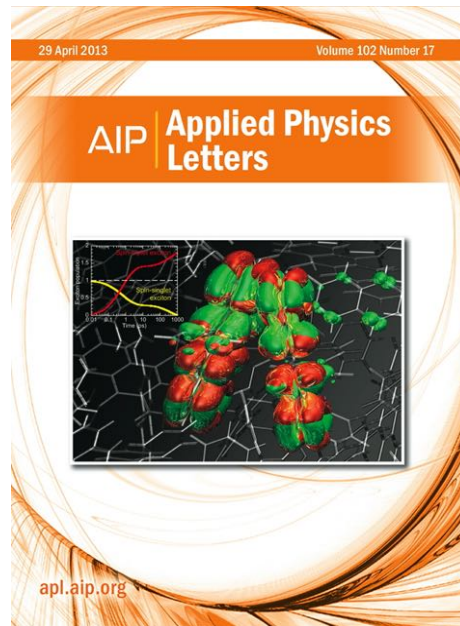
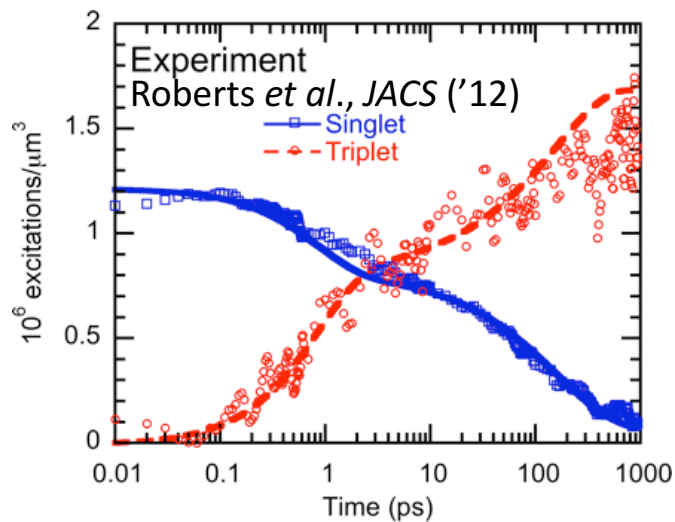
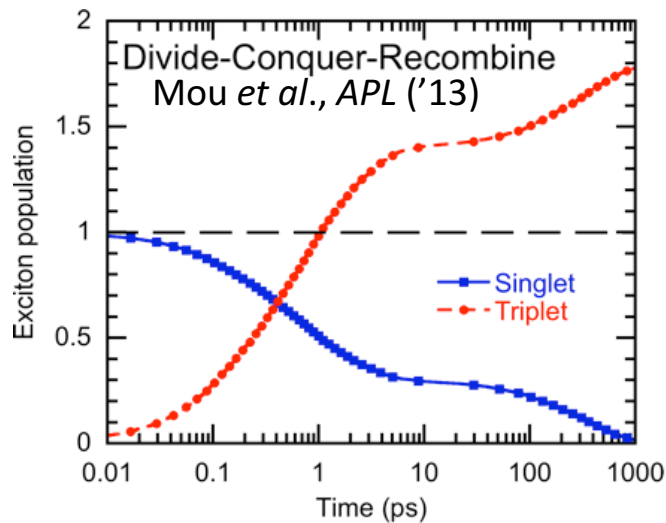
Quasi-electron

Quasi-hole

- **Divide-conquer-recombine nonadiabatic QMD** (phonon-assisted exciton dynamics) + time-dependent perturbation theory (singlet-fission rate) + kinetic Monte Carlo calculations of exciton population dynamics in **6,400-atom** amorphous DPT

Singlet-Fission Hot Spot

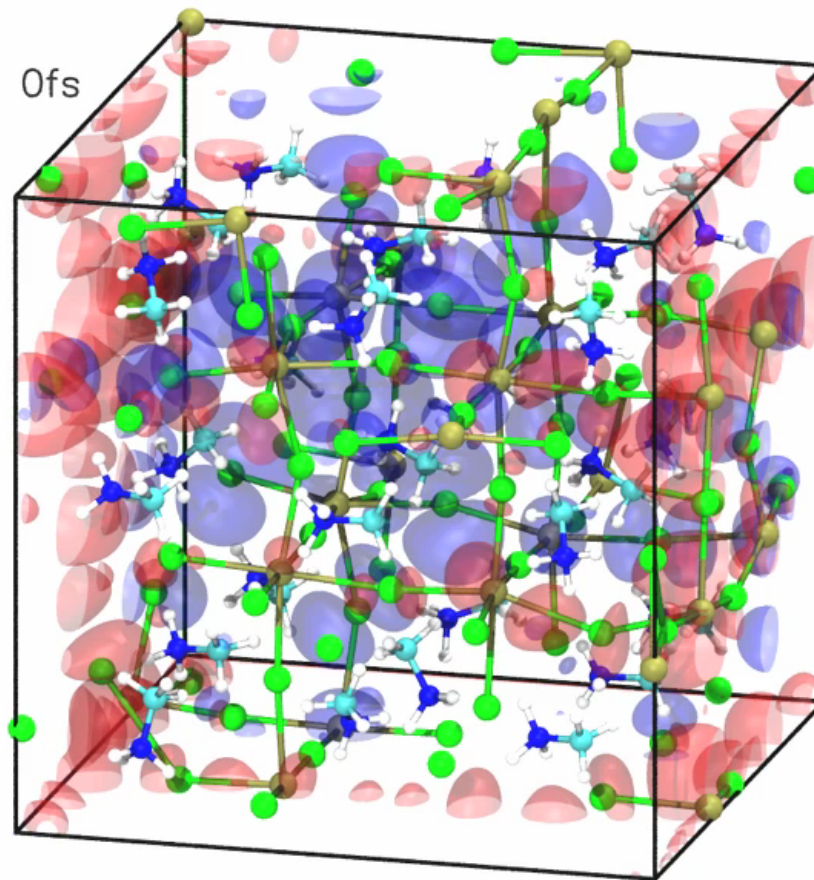
- **Nonadiabatic quantum molecular dynamics simulations not only reproduced experimentally measured exciton population dynamics but also revealed unknown molecular geometry of singlet fission hot spots**



Photoexcited Carriers in MAPbI₃

- **Organometal halide perovskites (e.g. methylammonium lead iodide, CH₃NH₃PbI₃ or MAPbI₃) for solar cells with high power conversion efficiency > 20%**

[Stranks & Snaith, *Nat. Nanotechnol.* **10**, 391 ('15)]



Quasi-electron
Quasi-hole
H, C, N, I, Pb

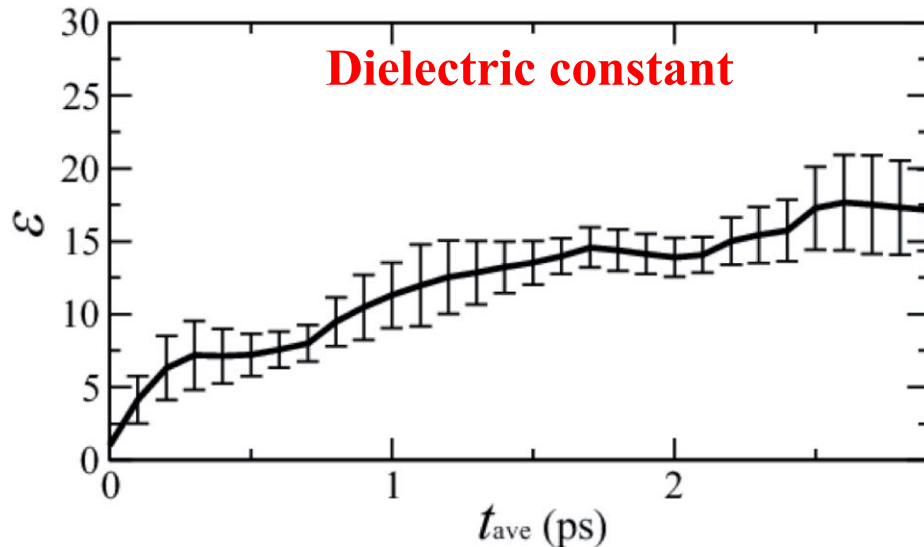
- **Nonadiabatic QMD simulation**

Pb & I sublattices act as disjunct pathways for rapid & balanced transport of free electrons & holes — electron (63% Pb-6p) & hole (90% I-5p);

diffusion coefficients $D_e = (1.16 \pm 0.31) \times 10^{-2} \text{ cm}^2/\text{s}$ & $D_h = (1.01 \pm 0.42) \times 10^{-2} \text{ cm}^2/\text{s}$

Expt: $D_e = (1.7 \pm 1.1) \times 10^{-2} \text{ cm}^2/\text{s}$ & $D_h = (1.1 \pm 0.7) \times 10^{-2} \text{ cm}^2/\text{s}$ [Stranks *et al.*, *Science* **342**, 341 ('13)]

Screening Role of Methylammonium Sublattice

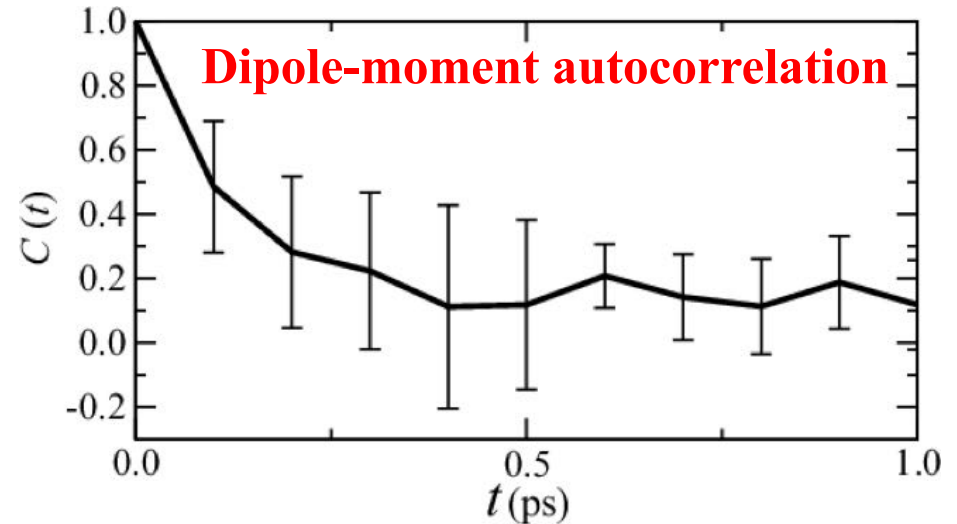


$$\epsilon = 1 + \frac{4\pi}{3k_BTV} (\langle \mathbf{M}^2 \rangle - \langle \mathbf{M} \rangle^2)$$

time average
dipole moment

cf. $\epsilon_{\text{expt}} (10^{12} \text{ Hz}) = 7\text{-}10$

Lin *et al.*, *Nat. Photonics* **9**, 106 ('15)



$$C(t) = \frac{\langle \mathbf{M}(t + t_0) \cdot \mathbf{M}(t_0) \rangle}{\langle \mathbf{M}(t_0) \cdot \mathbf{M}(t_0) \rangle}$$

Rapid response time ~ 1 ps

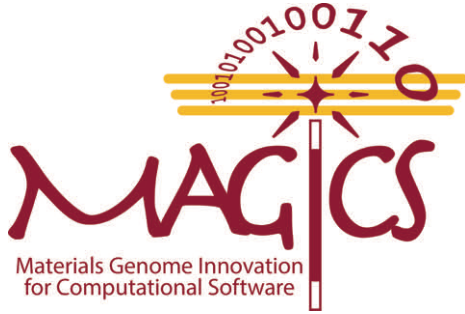
cf. $\tau_{\text{expt}} = 2 \text{ ps}$

Deschler *et al.*, *JPLCL* **5**, 1421 ('15)

- **Large dielectric constant of MA sublattice causes small exciton binding energy, $0.012 \pm 0.009 \text{ eV}$ (experimental upper bound = 0.05 eV [D'Innocenzo *et al.*, *Nat. Commun.* **5**, 3586 ('14)])**
- **MA sublattice quickly screens out electrostatic electron-hole attraction to unbind an exciton & generate free carriers within 1 ps** [cf. Zhu *et al.*, *Science* **353**, 1409 ('16)]

Hakamata *et al.*, *Sci. Rep.* **5**, 19599 ('16)

Materials Genome Innovation for Computational Software



U.S. DEPARTMENT OF
ENERGY

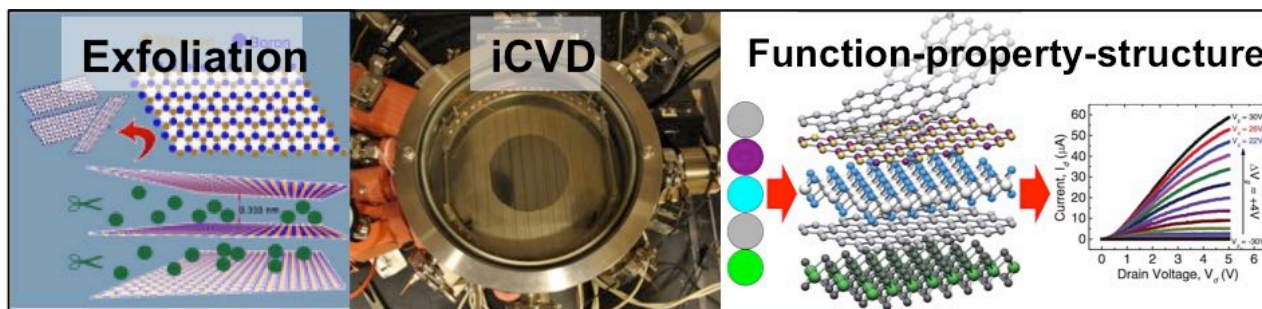
Office of
Science

Basic Energy Sciences

Priya Vashishta-PI, Malancha Gupta, Rajiv K. Kalia, Aiichiro Nakano, Oleg Prezhdo *University of Southern California*
Uwe Bergmann and David Fritz *Linac Coherent Light Source, SLAC*
William A. Goddard, III *California Institute of Technology*
Kristin A. Persson *Lawrence Berkeley National Laboratory*
David J. Singh *University of Missouri*
Pulickel M. Ajayan *Rice University*

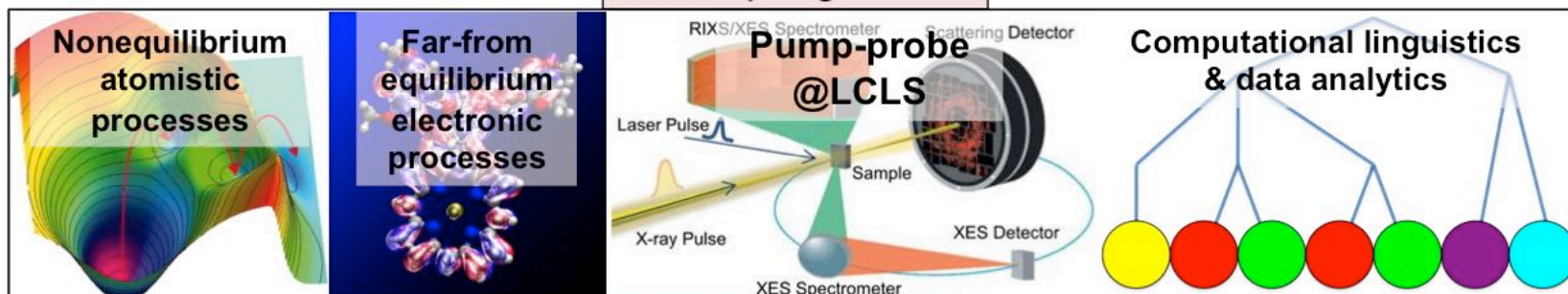


Computational Synthesis of Functional Layered Materials: MAGICS Software Stack



③ Extensible plug-ins – Computational synthesis

Scripting API



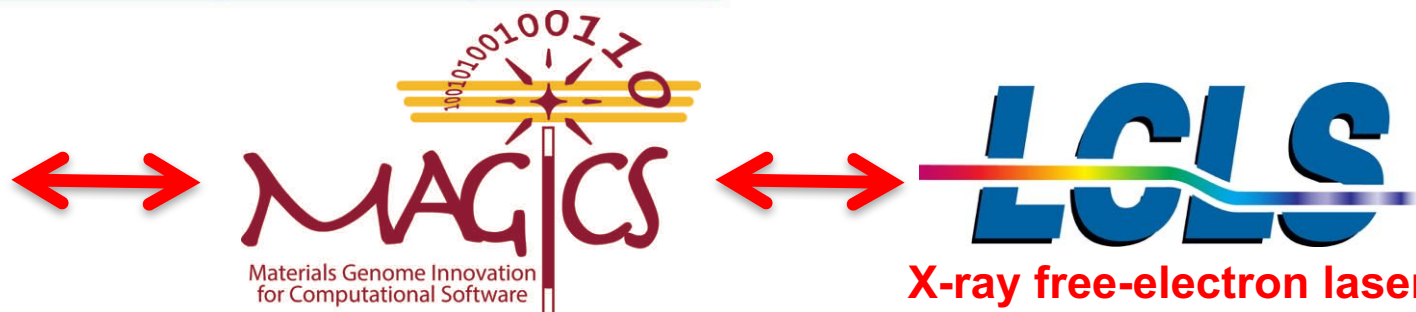
② Core libraries – Elementary processes

①

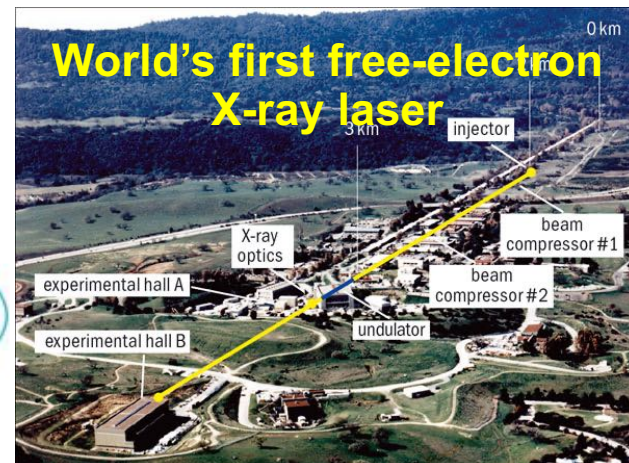
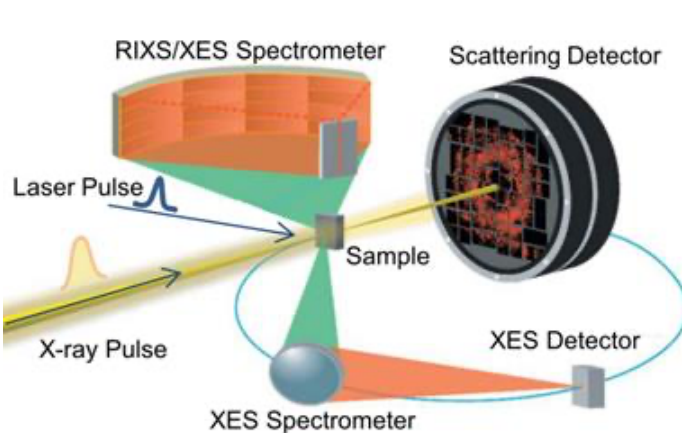
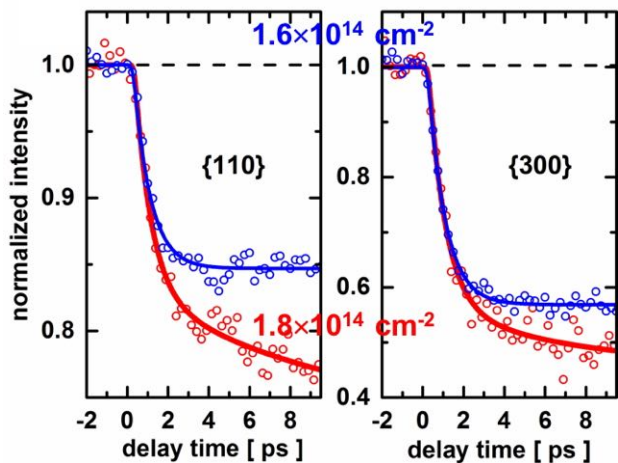
Scalable simulation engines

NAQMD	RMD	AMD
MPI	OpenMP	CUDA/Phi

Current/future platforms



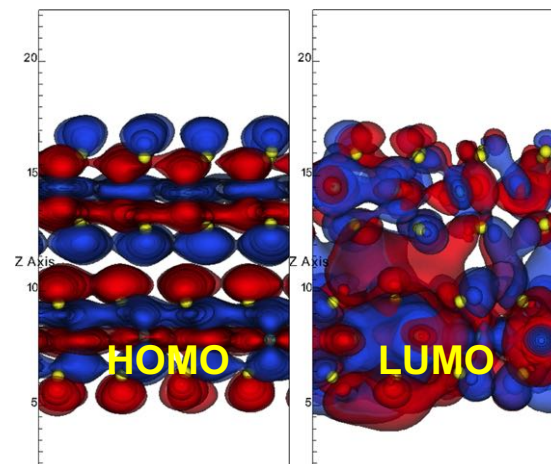
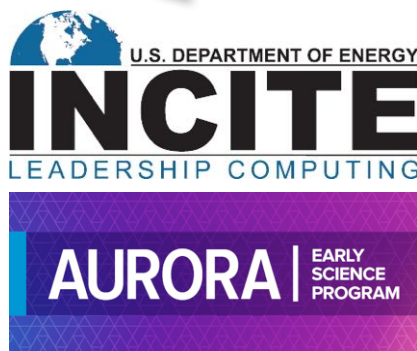
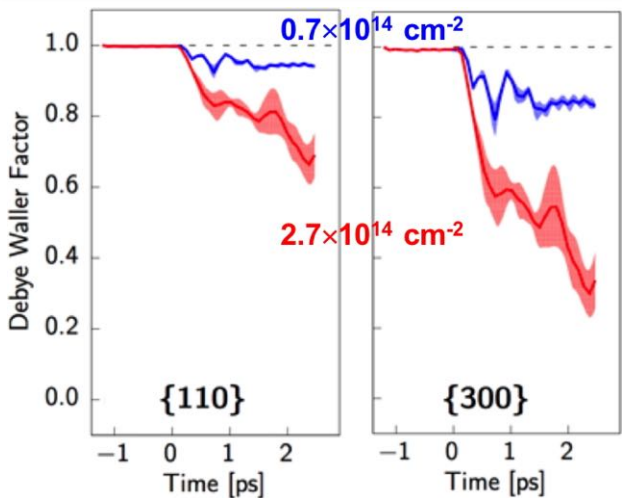
INCITE/AURORA-MAGICS-LCLS Synergy



Linac Coherent Light Source

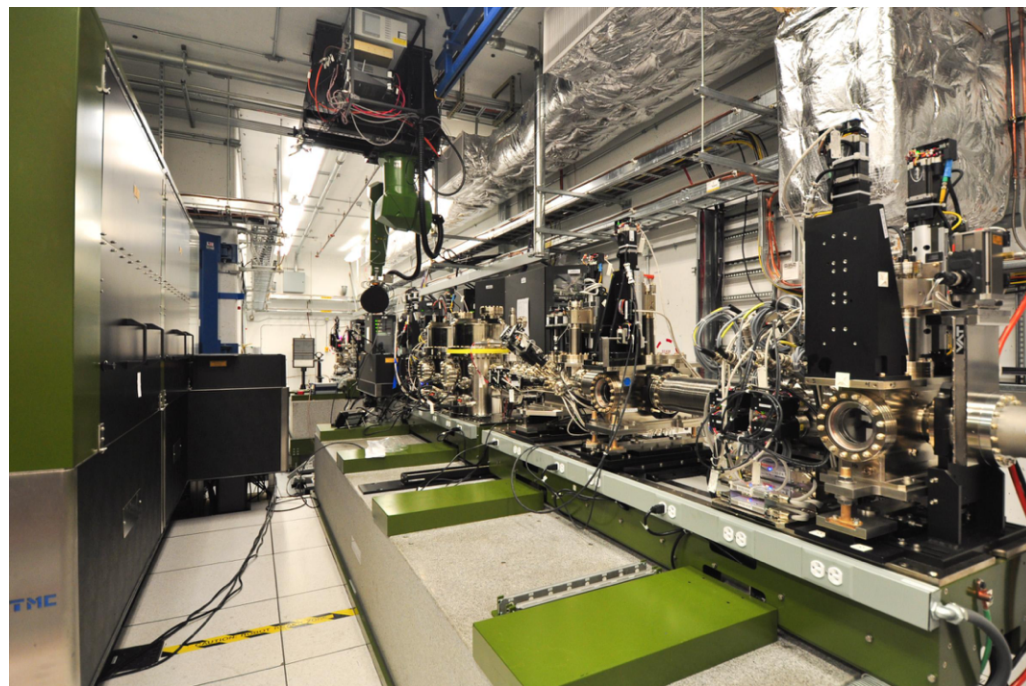


DOE INCITE & Aurora ESP Awards

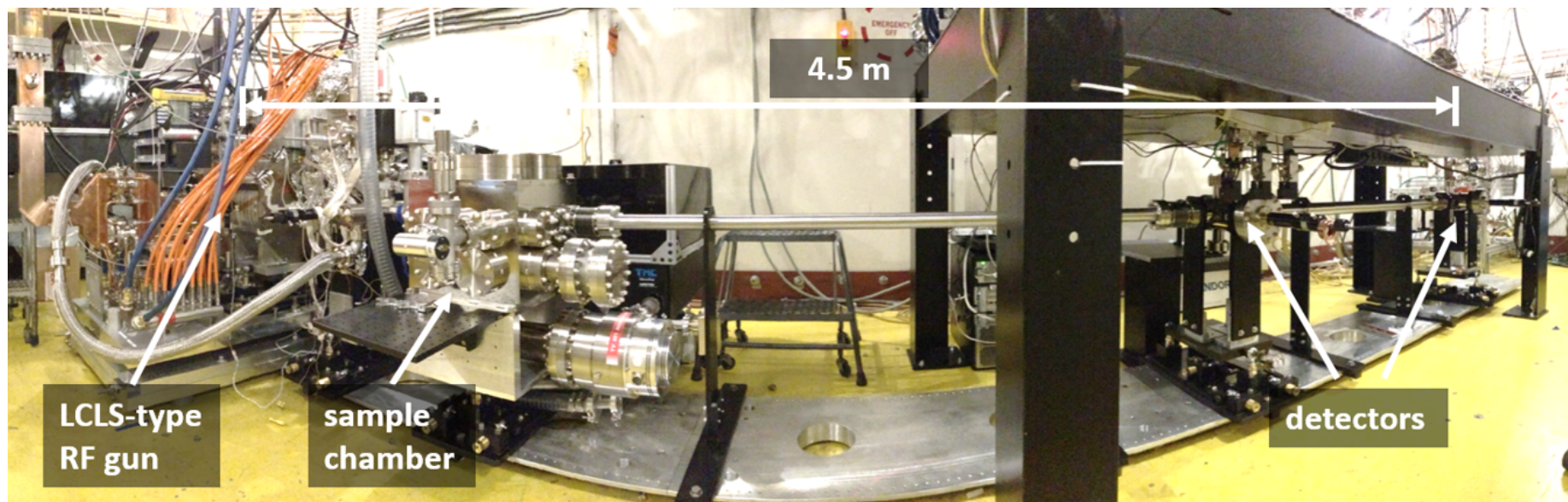


ULTRAFAST PUMP-PROBE EXPERIMENTS

X-ray pump-probe (XPP)
instrument: 4-25 KeV

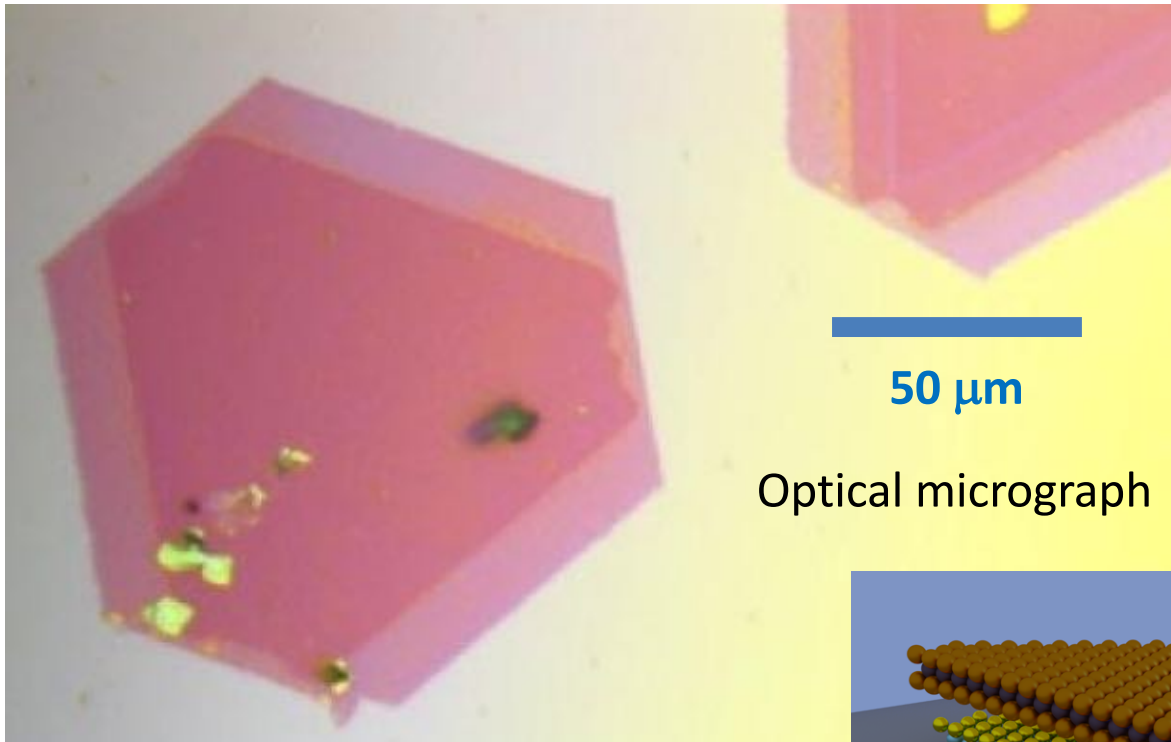


Ultrafast electron diffraction (UED)
instrument: 3-5 MeV

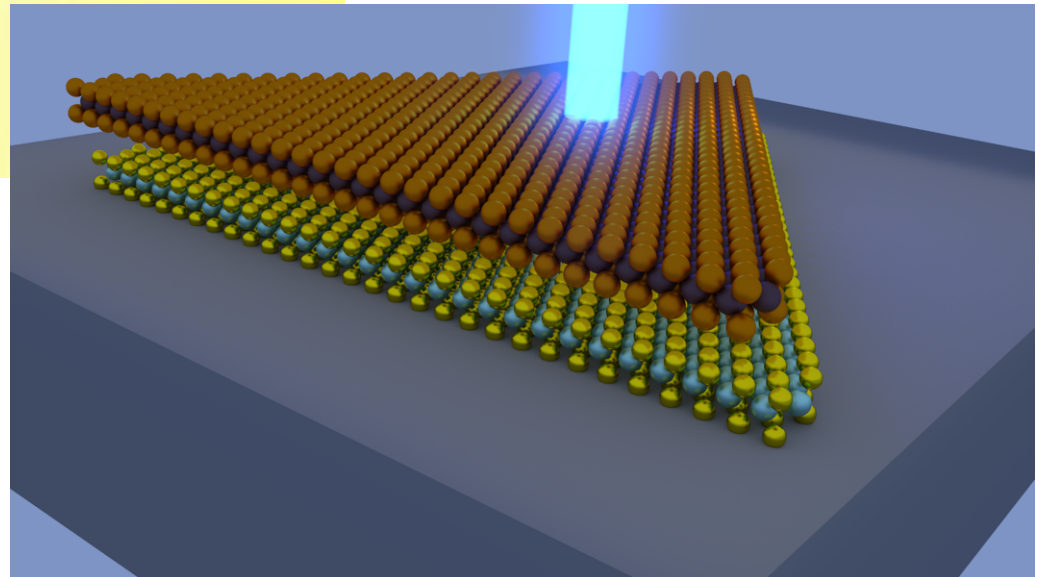


2D Transition Metal Dichalcogenide (TMDC)

- Mono- and bi-layer MoSe₂ synthesized by the Rice group (P. Ajayan)

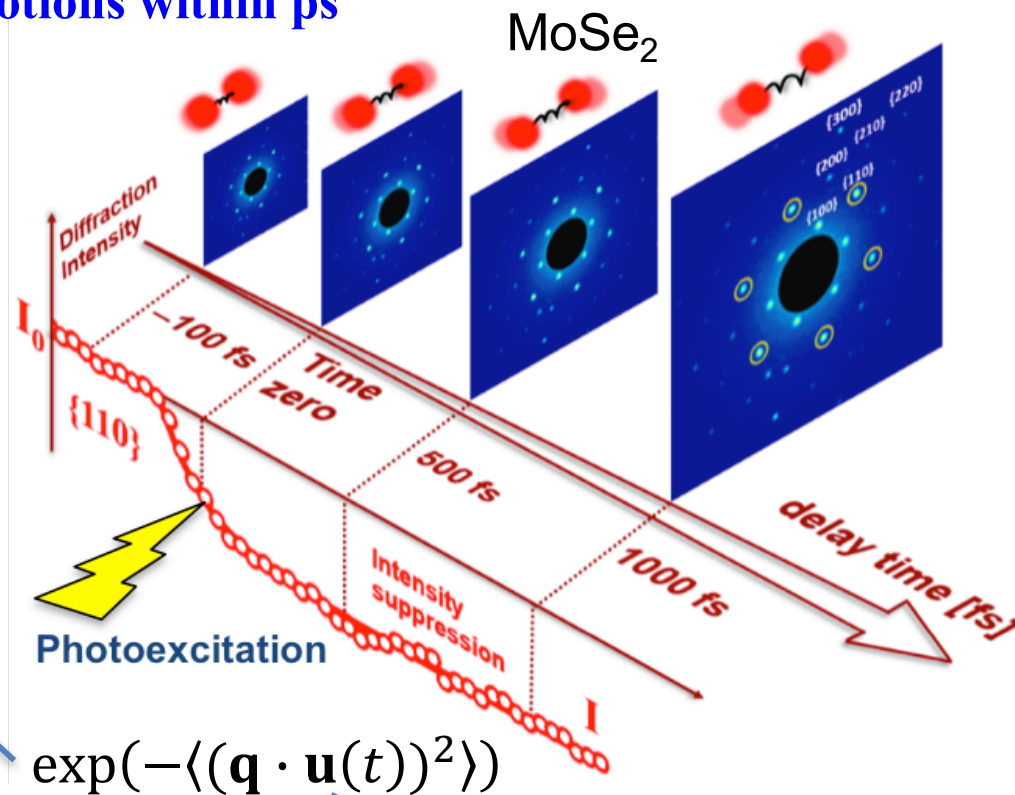
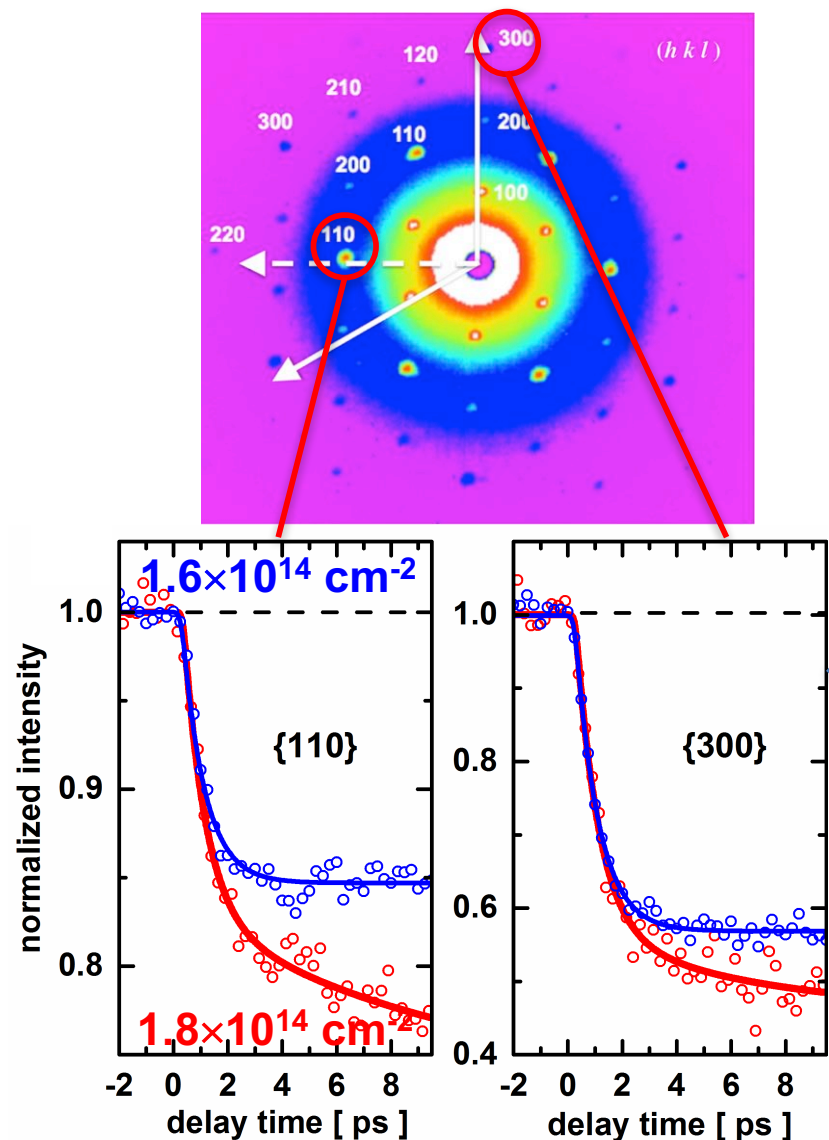


- **Question:** What is the nature of optically induced lattice dynamics for photo-patterning (e.g., semiconducting 2H to metallic 1T' phases) of TMDC?



Ultrafast Coupled Electron-Lattice Dynamics

- Ultrafast electron diffraction experiment shows nearly perfect energy conversion from electronic excitation to lattice motions within ps



$$\exp(-\langle (\mathbf{q} \cdot \mathbf{u}(t))^2 \rangle)$$

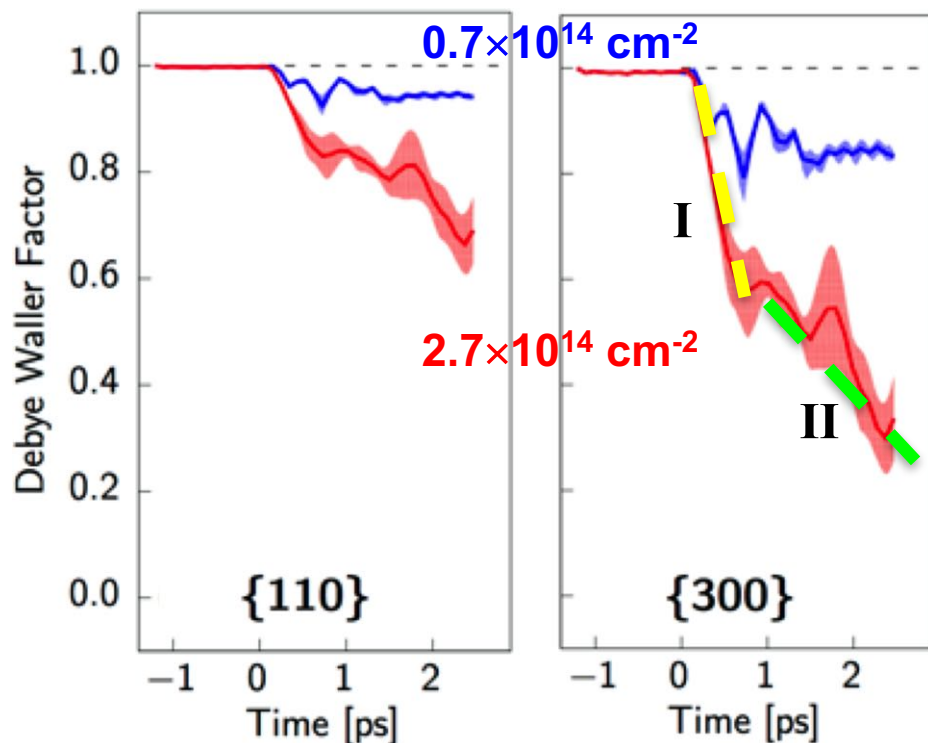
atomic displacement

- Dynamics of Debye-Waller factor reveals rapid disordering for both {300} & {110} peaks
- Transition from mono- to bi-exponential decay at higher electron-hole density

M.F. Lin *et al.*, *Nature Commun.* **8**, 1745 ('17)

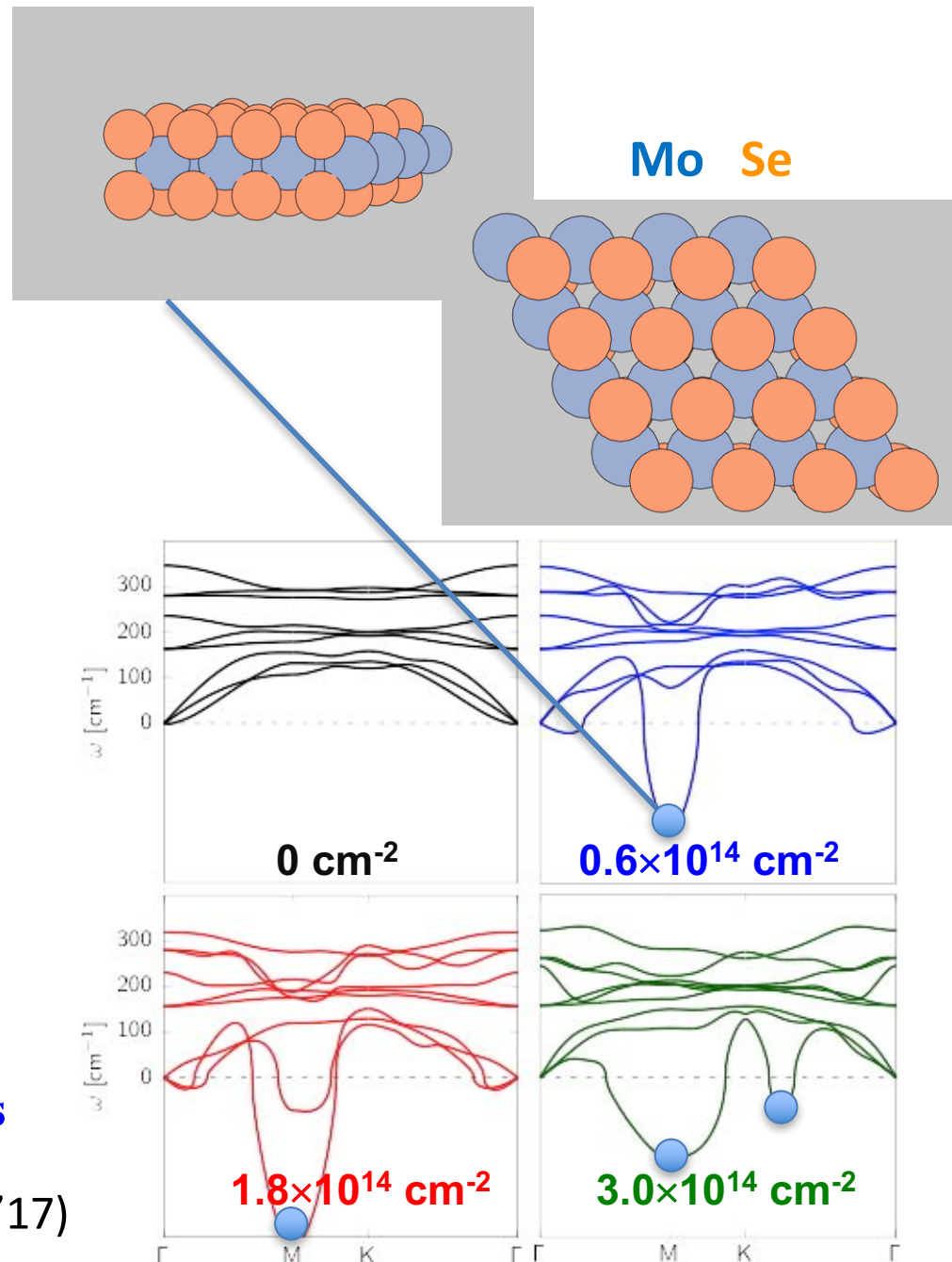
Strong Electron-Lattice Coupling

- NAQMD simulations reproduce (1) rapid photo-induced lattice dynamics & (2) mono- to bi-exponential transition at higher electron-hole density



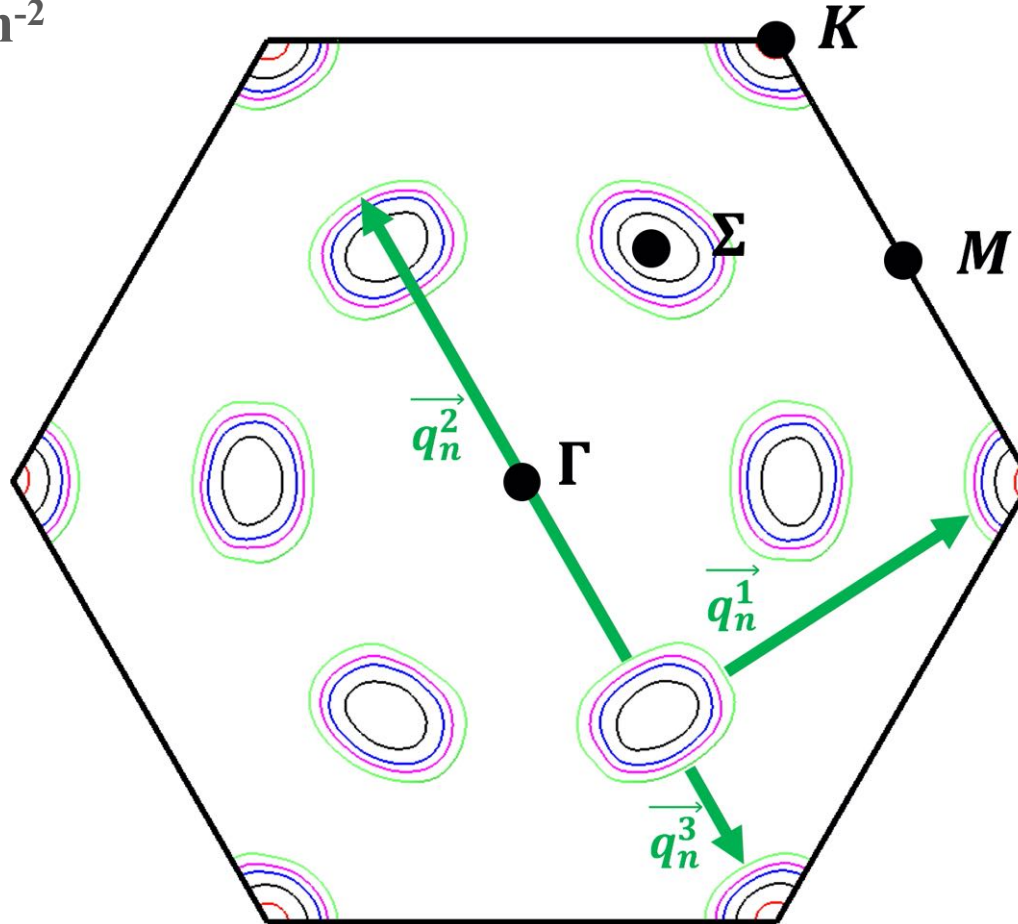
- Rapid lattice dynamics is explained by the softening of M-point ($1/2 \ 0 \ 0$) phonon
- Bi-exponential transition is explained by the softening of additional phonon modes at higher electron-hole densities

M.F. Lin *et al.*, *Nature Commun.* **8**, 1745 ('17)



Electronic Origin of Phonon Softening

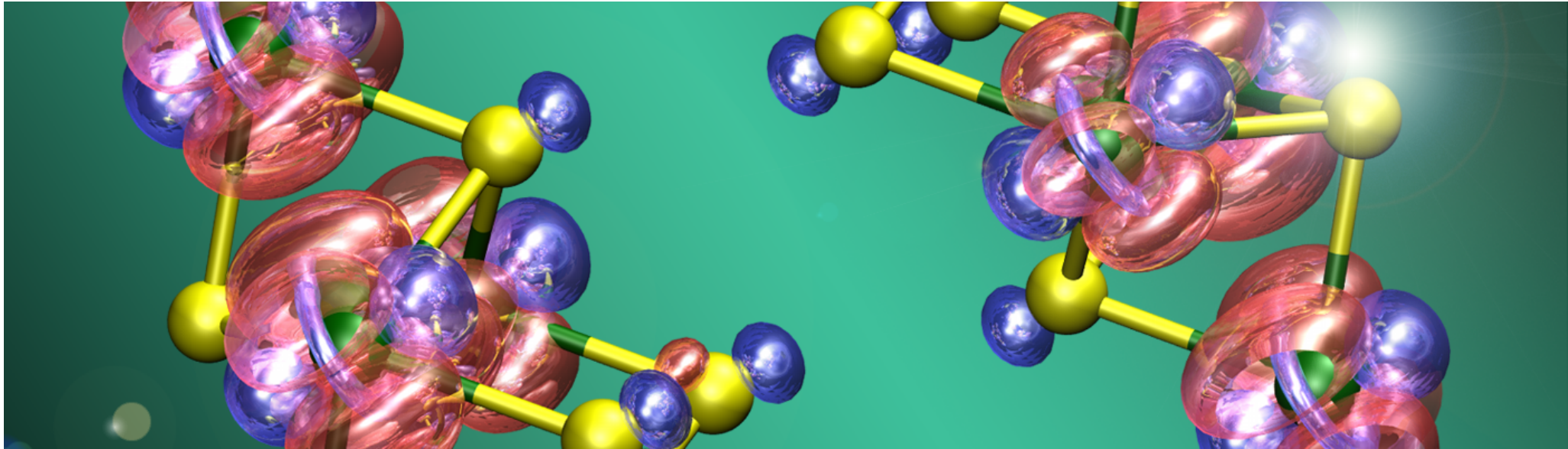
- Electronic Fermi surface for the electron-hole density $n(\text{e-h})$ ranging from 0.2 to $2 \times 10^{14} \text{ cm}^{-2}$



$$n(\text{e-h}) = 0.22, 1, 2, 3, 4 \times 10^{14} \text{ cm}^{-2}$$

- While the Fermi surface is localized at K -points at minimal excitation (red), it occupies Σ -pockets at larger $n(\text{e-h})$ (black & blue), enabling electron scattering by emitting \vec{q}_n^1 (M), \vec{q}_n^2 (Σ) and \vec{q}_n^3 (K) phonons

Simulation-Experiment Synergy

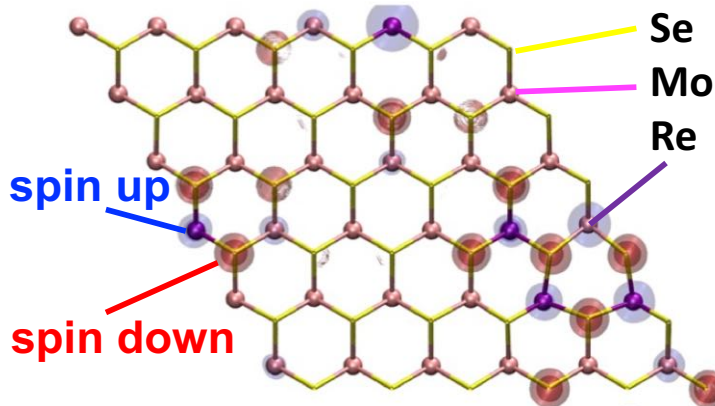
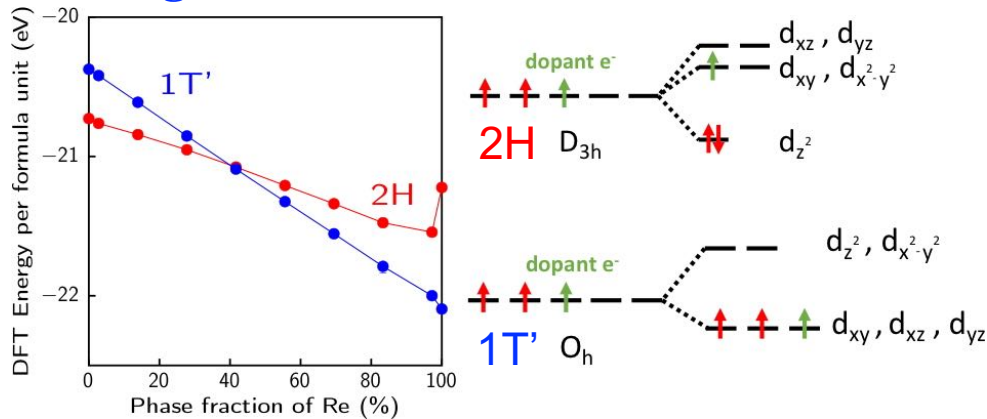


- In the ultrafast ‘electron camera,’ laser light hitting a material is almost completely converted into nuclear vibrations — key to switching material properties on & off at will for future electronics applications
- High-end quantum simulations reproduce the ultrafast energy conversion at exactly the same space & time scales, & explain it as a consequence of photo-induced phonon softening

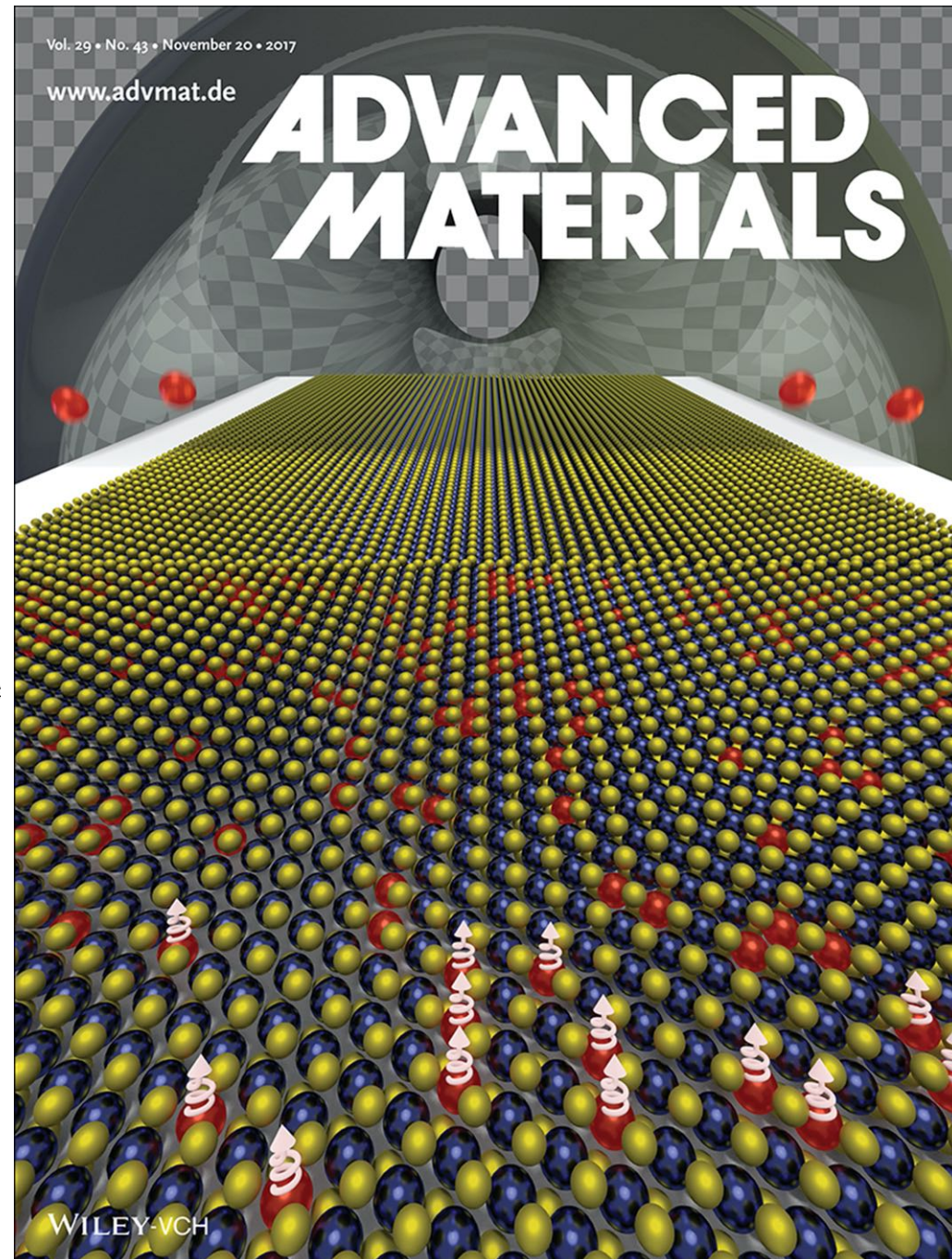
M.F. Lin *et al.*, *Nature Commun.* **8**, 1745 ('17)

Semiconductor-to-Metal Transition *via* Doping

- Experiment at Rice shows 2H-to-1T' phase transformation by alloying MoSe₂ with Re
- QMD simulations at USC elucidate its electronic origin
- Simulation & experiment show novel magnetism centered at Re atoms



V. Kochat *et al.*, *Adv. Mater.* **29**, 1703754 ('17)



Conclusion

1. Large spatiotemporal-scale quantum molecular dynamics simulations enabled by divide-conquer-recombine
2. Broad materials & energy applications

